The Tribbles 2 (TRB2) pseudokinase binds to ATP and autophosphorylates in a metal-independent manner

Fiona P. Bailey*, Dominic P. Byrne*, Krishnadev Oruganty†, Claire E. Eyers*, Christopher J. Novotny‡, Kevan M. Shokat‡, Natarajan Kannan†§ and Patrick A. Eyers*[1]

*Department of Biochemistry, Institute of Integrative Biology, University of Liverpool, Liverpool L69 7ZB, U.K.
†Institute of Bioinformatics, University of Georgia, Athens, GA 30602, U.S.A.
‡Department of Cellular and Molecular Pharmacology, Howard Hughes Medical Institute, UCSF, San Francisco, CA 94158, U.S.A.
§Department of Biochemistry and Molecular Biology, University of Georgia, Athens, GA 30602, U.S.A.

The human Tribbles (TRB)-related pseudokinases are CAMK (calcium/calmodulin-dependent protein kinase)-related family members that have evolved a series of highly unusual motifs in the 'pseudocatalytic' domain. In canonical kinases, conserved amino acids bind to divalent metal ions and align ATP prior to efficient phosphoryl-transfer to substrates. However, in pseudokinases, atypical residues give rise to diverse and often unstudied biochemical and structural features that are thought to be central to cellular functions. TRB proteins play a crucial role in multiple signalling networks and overexpression confers cancer phenotypes on human cells, marking TRB pseudokinases out as a novel class of drug target. In the present paper, we report that the human pseudokinase TRB2 retains the ability to both bind and hydrolyse ATP weakly *in vitro*. Kinase activity is metal-independent and involves a catalytic lysine residue, which is conserved in TRB proteins throughout evolution alongside several unique amino acids in the active site. A similar low level of autophosphorylation is also preserved in the closely related human TRB3. By employing chemical genetics, we establish that the nucleotide-binding site of an 'analogue-sensitive' (AS) TRB2 mutant can be targeted with specific bulky ligands of the pyrazolo-pyrimidine (PP) chemotype. Our analysis confirms that TRB2 retains low levels of ATP binding and/or catalysis that is targetable with small molecules. Given the significant clinical successes associated with targeting of cancer-associated kinases with small molecule inhibitors, it is likely that similar approaches will be useful for further evaluating the TRB pseudokinases, with the translation of this information likely to furnish new leads for drug discovery.

Key words: adenosine 5′-triphosphate (ATP), chemical biology, kinase, pseudokinase, Tribbles, Tribbles 2 (TRB2/TRIB2), thermo-stability assay (TSA).

INTRODUCTION

Protein pseudokinases are key components of all vertebrate kinomes and are defined as lacking at least one of the conserved motifs that are required for efficient ATP binding and/or catalysis in their canonical counterparts [1–3]. Pseudokinases are distributed throughout the human kinome with relative parsimony [3], suggesting that pseudokinase signalling, which extends to both prokaryotes [4] and primordial eukaryotes [5], is of relevance to both serine-/threonine- and tyrosine-related kinase homologues [6,7]. Until recently, biochemical analysis of human pseudokinases was neglected, although it is now appreciated that these proteins play a diverse mixture of catalytic and non-catalytic ('scaffolding') roles in an expanding range of cell signalling pathways [8]. Many human pseudokinases, including CASK (calcium/calmodulin-dependent serine protein kinase) [9], HER3 (human epidermal growth factor receptor 3) [10], JAK2 (Janus kinase 2; which also contains a canonical kinase domain in the same polypeptide) [11] and KSR1/2 (kinase suppressor of ras 1 and 2) [12], have retained a range of affinities for ATP that can be converted into weak catalytic activity in the pseudokinase active site *in vitro*, although the function of such 'vestigial' activities remains controversial in a cellular context [13]. However, although the concentration of ATP in cells is tightly buffered under normal conditions, it is present at low (∼1–5) millimolar concentrations [14], suggesting that kinases and pseudokinases with a demonstrable nucleotide affinity in this range [15,16] might be competent for nucleotide-mediated signal transduction in cells.

Recent work has begun to shed light on generalized aspects of pseudokinase biochemistry and structural biology [8,13,17–23]. An important example is the CAMK (calcium/calmodulin-dependent protein kinase)-family pseudokinase CASK, which lacks canonical metal-binding residues such as an aspartic acid in the DFG motif, but nonetheless possesses affinity for fluorescent TNP (trinitrophenol)-ATP and phosphorylates both itself and the specific substrate neurexin in a metal-independent manner *in vitro* [9]. Logical 'back' mutation of conserved non-canonical CASK amino acids leads to reinstatement of efficient metal-activated kinase activity, suggesting that CASK has evolved an atypical pseudokinase domain in order to regulate a specific function in the cell [24]. The four human Tribbles (TRB)-related pseudokinases [25] termed in the present study, TRB1, TRB2, TRB3 and SgK495 (sugen kinase 495), also lie in the CAMK sub-family and are most closely related to the *Drosophila* TRB pseudokinase, which controls targeted ubiquitination and degradation of specific transcription factors that co-ordinate cell cycle and morphogenesis in a pseudokinase domain-dependent manner [26–30].

The defining features of vertebrate TRB proteins are a central pseudokinase domain lacking canonical metal-binding amino acids and a conserved C-terminal motif that engages the ubiquitin E3 ligase machinery [31], although how this event is coupled to the pseudocatalytic core of TRB polypeptides remains unknown. Together, TRB proteins have been shown to regulate and drive several canonical signalling pathways that impinge on cell proliferation, viability and metabolic output [32]. In TRB2, expression is closely associated with several cancer-sustaining transcriptional programmes [32,33], and this is underpinned by the finding that TRB1 and TRB2 overexpression can independently drive acute myeloid leukaemia in mouse models of cancer [33,34]. Interestingly, cellular transformation by human TRB2 is dependent on an intact ATP-binding site [35], suggesting that ligands capable of modifying TRB2 signalling output might have utility as drugs in cases where TRB2 overexpression is causative for disease development or maintenance. Additionally, TRB3 (and TRB2) are implicated as regulators for Notch signalling and TRB3 is also a prognostic factor in breast cancer [36,37]. No structural information for TRB pseudokinases is currently available, and a key bottleneck in advancing the TRB field in particular and for pseudokinase analysis in general is a lack of suitable assays, reagents and small molecule probes. This currently restricts our ability to investigate cellular functions of pseudokinases, a key prerequisite to their evaluation as disease targets. Since ATP-dependent small molecule ligands remain central to this quest, a thorough knowledge of the nucleotide-binding potential of pseudokinases such as TRB2 is also required to support chemical biology and drug discovery efforts.

To instigate a molecular analysis of TRB proteins, we overexpressed human affinity-tagged TRB2 in bacteria and purified it to homogeneity, optimizing buffer conditions that promote TRB2 stability. This permitted the first comparative biochemical analysis to be performed for TRB2 in vitro. In the present paper, we report that, despite the absence of several canonical residues, TRB2 retains the ability to bind with low affinity to ATP in a manner reliant upon the canonical $\beta3$ lysine residue (Lys^{90}), which is conserved in all TRB pseudokinases. Moreover, like CASK, TRB2 autophosphorylates independently of various divalent metal ions in vitro. A low level of autophosphorylation is also associated with TRB3, suggesting a generalized preservation of nucleotide-dependent phosphotransfer in TRB pseudokinases, although specific TRB substrates have not yet been identified. Finally, we confirm the druggability of the TRB2 pseudocatalytic site by investigating the binding of a panel of bulky small molecule ligands to an 'analogue-sensitive' (AS) TRB2 mutant in which the gatekeeper amino acid is mutated to a small alanine or glycine residue. Taken together, our study confirms a vestigial kinase activity in several TRB pseudokinases and opens up the ATP-binding site of this and potentially other human pseudokinases for further scrutiny.

EXPERIMENTAL

Bioinformatic analysis of Tribbles pseudokinases

Human protein kinase domain boundaries [3,38] or the complete sequences of 17 TRB2 eukaryotic orthologues, were obtained from the UniProt database and alignments and secondary structure predictions were performed using the JalView bioinformatics suite [39]. TRB-related pseudokinase domain cancer mutations that occurred at the same site independently on more than one occasion were retrieved for TRB1, TRB2, TRB3 and SgK495 from v.71 of COSMIC (catalogue of somatic mutations in cancer) [40] and mapped to protein kinase A (PKA) using the protein

kinase ontology [41,42]. The location and frequency of combined mutations in the TRB pseudokinase domains are represented by the relative volume of the red spheres. The alignment of TRB2 and related sequences was performed using curated profiles as described previously [43].

Cloning and recombinant protein production in bacteria and Sf9 cells

Full-length cDNAs encoding the human pseudokinases TRB2 (1–343), TRB3 (1–358), SgK495/STK40 (Ser/Thr kinase 40) (1–435), STRADα (STE20-related kinase adapter protein alpha) (1–431), CASK (amino acids 1–337 containing the complete CAMK-like domain) or full-length Aurora A or a kinase-inactive mutant in which the aspartic acid in the DFG motif was mutated to prevent ATP binding (D^{274}N) were cloned into the bacterial expression vector pET-30 Ek/LIC (ligation-independent cloning), which encodes an N-terminal His$_6$ tag as part of a 43 amino acid extension that is compatible with TSAs (thermo-stability assays) to analyse ligand binding. In addition, CASK was cloned into the pET-41 Ek/LIC vector, which encodes a GST and His$_6$ tag at the N-terminus to aid solubilization and rapid affinity purification for kinase assays, as previously described [24]. Point mutations, including TRB2 K^{90}A, K^{90}R, K^{90}M, K^{177}A, K^{180}N, K^{180}N:S^{195}D:L^{196}F:E^{197}G and TRB3 K^{97}M were generated by PCR and specific mutations were confirmed by automated DNA sequencing of the entire cDNA. All recombinant human proteins were expressed in the Escherichia coli strain BL21(DE3) pLysS (Novagen) with induction in 0.5 mM ITPG at 18°C for 18 h, as described previously [44]. The cDNA of full-length human TRB2, K^{90}M and the quadruple mutant K^{180}N:S^{195}D:L^{196}F:E^{197}G were also cloned into pBAC-2cp Ek/LIC (Novagen), which encodes an N-terminal His$_6$ tag and recombinant proteins were subsequently purified from Sf9 cells after virus amplification, transfection and expression optimization.

Protein purification, buffers and TRB2 analysis

The proteins analysed in the present study all contain an N-terminal His$_6$ tag, permitting partial purification by immobilized metal affinity chromatography (IMAC) directly from the bacterial extract. All proteins were expressed and purified from bacteria and processed as described previously [44], with yields of between ~1 mg (SgK495, TRB3), ~5 mg (STRADα) and ~10 mg (TRB2, CASK and Aurora A) of purified protein obtained per litre of Luria–Bertani (LB) medium. Extracts were applied to an Ni-Sepharose column and eluted in 50 mM Tris/HCl, pH 7.4, 300 mM NaCl, 300 mM imidazole, 1 mM DTT and 10% (v/v) glycerol. Prior to analysis, proteins were buffer exchanged into a standard TRB buffer [20 mM bicine, pH 9.0, 100 mM NaCl, 1 mM DTT and 10% (v/v) glycerol], after which they were snap frozen in liquid nitrogen and stored at − 80°C. TRB2 dispersity was analysed by size exclusion chromatography–multi-angle laser light scattering (SEC–MALLS) in TRB buffer.

SDS/PAGE and immunoblotting

After assay, proteins were denatured in Laemmli sample buffer, heated at 95°C for 5 min and then analysed by SDS/PAGE with 12% (v/v) polyacrylamide gels. Gels were stained and destained using a standard Coomassie Brilliant Blue protocol and dried prior to autoradiography and quantification. To evaluate proteins by immunoblotting, standard Western blotting procedures were followed. Recombinant bacterial His–TRB2, His–TRB3 and Sf9-derived TRB2 were all immunblotted with an anti-poly-histidine antibody conjugated to horseradish peroxidase (HRP) (Sigma) in the presence of appropriate positive and

negative controls, and protein was visualized using enhanced chemiluminescence (ECL) reagent.

^{32}P-based kinase assays

To investigate whether a panel of pseudokinases and kinases could autophosphorylate, affinity-purified TRB2, GST–CASK, SgK495, STRADα, D^{274}N Aurora A or wild-type (WT) Aurora A were dialysed into standard TRB-stabilizing buffer [20 mM bicine, pH 9.0, 100 mM NaCl, 1 mM DTT and 10% (v/v) glycerol] and 250 pmol (∼12 μg) of TRB2, CASK, SgK495, STRADα or D^{274}N Aurora A or 25 pmol (1.25 μg) of WT Aurora A, were assayed at 30°C on a shaking platform in the presence of 1 mM ATP (∼2.5 μCi of [γ^{32}P] ATP per assay total) and 2 mM EDTA, or 10 mM MgCl$_2$ in the absence of EDTA (WT Aurora A). Where appropriate, the indicated concentration of Mg^{2+} ions were added prior to ATP addition and TRB3 and TRB3 K^{97}M were assayed for 30 min alongside TRB2 and TRB2 K^{90}M with no metal ions added to each reaction in the presence of 2 mM EDTA and 1 mM ATP and ∼2.5 μCi [γ^{32}P] ATP per assay. The reactions were terminated at the indicated time-points by the addition of 5× SDS loading buffer and samples were heated to 95°C for a duration of 5 min. For analysis of $K_{m[ATP]}$ values using a Tris-based buffer at pH 7.4, 25 μCi of [γ^{32}P] ATP was employed at the highest concentration in the assay at a specific activity of ≥2000 cpm/pmol, utilizing 20 mM Tris/HCl, pH 7.4, 100 mM NaCl and 1 mM DTT. To evaluate incorporated radiolabelled phosphate, SDS/PAGE resolved TRB2 and CASK proteins were examined by autoradiography after 48–96 h of exposure to X-ray film. Quantification was performed by densitometric analysis, using appropriate Coomassie Blue-stained proteins resolved by SDS/PAGE using ImageJ (NIH) and/or by employing phosphorimager software analysis (Fuji FLA-3000). Non-linear regression analysis was used to calculate *in vitro* $K_{m[ATP]}$ values for autophosphorylated (^{32}P-label incorporation) TRB2 or CASK or Aurora A-phosphorylated histone H3 (activity calculated from scintillation-based counting of excised ^{32}P-gel bands and comparison with ATP of a known specific activity) using GraphPad Prism 6. To evaluate metal inhibition at pH 7.4, the effects of various divalent cations (10 mM) were analysed in 20 mM Tris/HCl, pH 7.4, 100 mM NaCl and 1 mM DTT. EDTA, EGTA, NaCl, MgCl$_2$, MnCl$_2$, Sr(NO$_3$)$_2$, CaCl$_2$, NiCl$_2$, CoCl$_2$ and CuSO$_4$ were all purchased from Sigma and 100 mM stock solutions were prepared prior to dilution into the appropriate assay.

MS

ESI–MS was performed using a Waters Q-TOF Global Instrument and a nano-electrospray, using gel-filtered TRB2 that eluted in the expected volume of the monomeric species. BSA was used as a standard and the data were deconvoluted using MAXENT1 software (Waters). The identity of the contaminating band co-purifying in SgK495 and STRADα preparations was confirmed using standard LC–MS procedures after in-gel trypsin digestion of the protein band.

Chemicals and compounds

All biochemicals, including bicine, LB, metal salts and antibiotics were purchased from either Melford or Sigma and were of analytical quality. [γ-^{32}P]ATP (5 mCi) was purchased from Perkin-Elmer and diluted appropriately with unlabelled ATP. Sypro Orange dye was from Invitrogen and was diluted as

described in the Invitrogen TSA protocol. A small compound library composed of 30 modified PP1 (pyrazolo-pyrimidine) analogues was prepared as previously described [45]. The compounds contain bulky additions at the C5 position of the pyrimidine ring that are designed to interact with the hydrophobic pocket adjacent to the gatekeeper residue of AS protein kinases. Compounds were stored at 10 mM in DMSO at −80°C until required and diluted directly into the assay at 250 μM, so that the final DMSO concentration was no higher than 2.5% (v/v) in any assay. Acronyms for compounds A, B and F are dClB-PP1 (A): dichlorobenzyl-PP1; dmB-PP1 (B): dimethylbenzyl-PP1; bisPh-PP1 (F): bisphenyl-PP1. Similar data were obtained from two independent compound preparations.

RESULTS

Bioinformatic analysis of the Tribbles 2 pseudokinase domain

No crystal structures of TRB pseudokinases are publicly available, although X-ray structures of several related CAMK-family members have been reported, including the pseudokinase CASK (PDB ID: 3C0G), which crystallizes in a conformation with high structural similarity to active PKA, PDB ID: 1ATP [9]. The highly unusual TRB2 pseudokinase domain was aligned with multiple model kinases (Figure 1A), including the fly orthologue TRB (kinase domain sequence identity of ∼40% with TRB2), TRB1 and TRB3 (72% and 55% sequence identity respectively), the more distantly related and highly unusual pseudokinase SgK495 (∼35% identity), the catalytically active pseudokinase CASK (28%) and the ATP-binding, but catalytically inactive, pseudokinase STRADα (∼20%). Also included in the alignment for comparative purposes were the kinase domain sequences of the canonical kinases CAMK1 (28% identity), PKA (23.6%) and CDK1 (cyclin-dependent kinase 1; 20.6% identity) whose mechanism of activation and catalysis are particularly well understood. In addition, we modelled the TRB2 pseudokinase domain sequence (Figures 1B and 1C) using a recent structure of the murine MELK (maternal embryo leucine zipper kinase) kinase domain (also included in the alignment) as a guide. MELK is the most closely related CAMK/AMPKα-related family member (31.3% sequence identity to human TRB2) for which an X-ray structure has been reported [46] and murine MELK (>98% identical to human) crystallizes in an active, closed conformation (PDB ID: 4BFM), and so was used as a template for our structural analysis (Figure 1B). The modelled β1-β2 loop (G-loop, blue in Figure 1B), which contains the GXGXXG motif in canonical kinases, such as PKA, is replaced by an acidic TRB 'signature' sequence (EPLEGD in TRB2, Figure 1A) and these side chains are predicted to protrude into the ATP-binding cleft, above the site of ATP binding found in canonical kinases. The highly conserved β3 strand lysine residue (Lys^{90}, cyan, equivalent to Lys^{72} of PKA) adopts a similar conformation to that seen in PKA, with the charged lysine pointing into the ATP-binding site. In PKA, Glu^{91} in the C-helix of PKA forms a well-defined salt bridge, with the β3 lysine residue (PKA Lys^{72}). In contrast, the orientation of a TRB2 glutamic acid residue (Figure 1B, Glu^{99} in orange) is predicted to point away from the cleft, making the formation of such a salt bridge unlikely in TRB2 despite the high conservation of Lys^{90} across all TRB pseudokinases. The predicted gatekeeper residue of TRB2 (Phe^{130}), which lies adjacent to a hydrophobic pocket not used by ATP is found at the end of the β4 strand in the N-lobe, where a pair of adjacent phenylalanine residues (Phe^{129} and Phe^{130}) are located. The predicted catalytic loop (yellow) and the TRB pseudokinase replacement for the Mg^{2+} ion-binding motif (red) are located
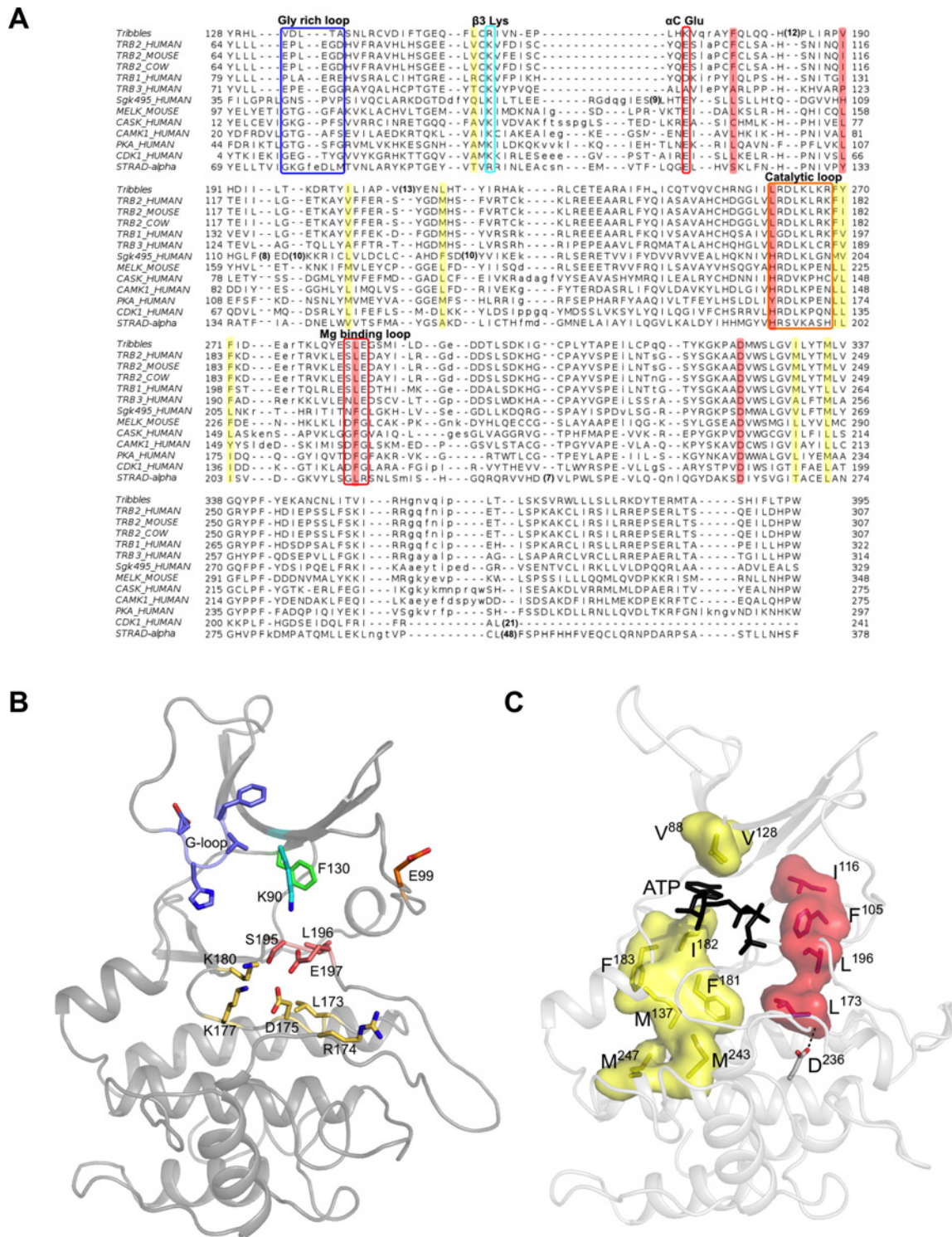
Figure 1   Alignment of the TRB2 pseudokinase domain with related (pseudo)kinases

(**A**) Kinase domain boundary sequences for fly TRB, human, murine and bovine TRB2, human TRB1, TRB3, SgK495, murine MELK, human CASK, PKA, CDK1 and STRADα were aligned using MUSCLE and JalView software, highlighting conserved and distinct regions among the canonical (pseudo)kinase domain motifs. The residues important for TRB2 ATP binding and hydrolysis are predicted based on comparison with the aligned PKA kinase domain. The TRB2 glycine-rich loop (blue), the conserved lysine residue of the β3 motif (cyan), the putative conserved glutamic acid in the C-helix (red), the catalytic loop (gold) and the Mg^{2+} ion-binding motif (red) can be inferred from alignments with the canonical kinase domains. Note that in TRB, TRB1, TRB2, TRB3 and SgK495, the glycine-rich loop lacks the GXGXXG consensus, and the terminal asparagine residue of the catalytic loop and the DFG Mg^{2+} ion-binding residues are not encoded within the polypeptide sequences of this family, a peculiarity also observed in part for the pseudokinase CASK (GFG motif). Residues that form the putative catalytic (C) and regulatory (R) spines are shaded in yellow or red respectively on the alignment. (**B**) Structural model of the pseudocatalytic site of TRB2, showing the disposition of a number of key amino acids, including the unusual glycine-rich loop, Lys[90], Asp[175] (the putative catalytic base), Lys[177] and Lys[180] (at the end of the catalytic loop) and residues Ser[195], Leu[196] and Glu[197], which replace the canonical DFG motif. (**C**) Model of hydrophobic C spine (yellow) and R spine (red) residues, assembly of which can potentially be driven by the conserved F-helix canonical aspartic acid residue that is conserved at position 236 in TRB2. Putative spine residues (corresponding to their PKA counterparts) are numbered and shown as space-filling.

within the C-lobe of the kinase domain and appear to line the ATP-binding cleft (Figure 1B).

Consistent with their close evolutionary origins, TRB, TRB1, TRB2, TRB3 and SgK495 (in particular) also lack key residues encoded within the kinase domain that bind to divalent cations in model kinases such PKA. In TRB2, the sequence SLE is predicted to replace the DFG motif, with a unique acidic glutamic acid residue residing at the -1 position and an aspartic acid residue at the $+1$ position. These residues are conserved in all TRB pseudokinases and across the full evolutionary spectrum of eukaryotic TRB2 homologues surveyed (Supplementary Figure S1). In addition, the catalytic loop lacks the near-invariant histidine of the HRD motif found in nearly all kinases, replacing this metal-centre-binding residue with a hydrophobic leucine (which cannot form a hydrogen bond) and terminating with a conserved lysine or arginine residue in TRB1, TRB2 and TRB3 instead of the canonical metal-binding asparagine residue found in most other kinases.

Sequence and structural modelling of the TRB2 polypeptide suggests the presence of several conserved hydrophobic residues in the positions that normally form the two distinct structural hydrophobic spines spanning the smaller N- and larger C-lobes of the kinase domain [47]. These spines terminate at the αF helix of PKA, and red shaded boxes show the putative TRB2 regulatory spine and yellow shaded boxes the putative TRB2 catalytic spine in Figure 1(C). This analysis suggests that these residues might readily come together to form an active ATP-trapped conformation in TRB2, stabilizing a domain structure compatible with catalysis [48]. Both TRB2 and TRB3, but not TRB1, also possess an RD sequence in their catalytic motifs (TRB2 Arg[174] Asp[175]) and RD kinases typically require phosphorylation of a residue within the activation segment to enhance their rate of catalysis [49]. In PKA, this residue is Thr[197], whereas in CDK1, it is Thr[161]. Interestingly TRB2 has a serine at the position that aligns with the CDK-activating threonine (TRB2 Ser[210]) and a charged aspartic acid residue (Asp[211]) at the equivalent position to Thr[197] of PKA.

Recombinant human TRB2 binds to ATP in the absence of metal ions

Previous work has established that many purified pseudokinase domains are unable to bind to nucleotides or metal cofactors when assayed using a standard set of experimental conditions [22]. Using this TSA protocol, TRB2 was only weakly stabilized by 0.2 mM ATP when analysed by Sypro Orange-based fluorescence (ΔT_{m} ~1 °C) and this subtle effect was thought to rule out *bona fide* ATP binding based on comparison with other kinases and pseudokinases in the panel [22]. However, cellular data suggest a potential role for the TRB2 pseudokinase domain in proliferation, since a conserved catalytic loop lysine residue (Lys[177]; Figure 1A) is required to support TRB2-dependent cell transformation, raising the possibility that an integral ATP-binding site might still be required in the intact TRB2 polypeptide. To evaluate this hypothesis more closely, we devised new protocols that allowed us to isolate and stabilize significant quantities of pure recombinant human TRB2 proteins from bacteria for biochemical analysis (Supplementary Figure S2). These screens, which employed modifications of previously published procedures [50], culminated in the discovery that a bicine (*N,N*-bis[2-hydroxyethyl]glycine) saline solution buffered at pH 9.0 and supplemented with 10 % (v/v) glycerol was optimal for TRB2 stability since it prevented protein aggregation and permitted freeze–thaw cycles without denaturation. Under these conditions, TRB2 was stable during purification and assay and

could be isolated in a stable monomeric, monodispersed form for analysis (Supplementary Figure S2). Except where stated explicitly, we have utilized these assay conditions at pH 9.0 throughout the present study.

Multiple fluorescence-based protocols are already in use for analysing ligand interactions with proteins and several of these have been adopted for protein kinase and pseudokinase analysis, whose wide variety of ATP affinities make them somewhat challenging to study and compare collectively [9,10,19,22,51–53]. In addition to detection of fluorescence from an extrinsic hydrophobic dye, the thermal stability of proteins can also be analysed by detecting the intrinsic fluorescence emitted by the indole ring of internal tryptophan residues as they become exposed to the solvent during denaturation [54]. We initially exploited this approach to measure intrinsic fluorescence changes associated with pseudokinase denaturation in the presence and absence of various ligands and cofactors. As shown in Figure 2(A), the T_{m} of TRB2 in the presence of EDTA increased by 3.64 °C in the presence of ATP. A ΔT_{m} value of 3–4 °C is usually indicative of a *bona fide* binding interaction [22], and as a control, the canonical kinase Aurora A exhibited a ΔT_{m} of 2.99 °C in the presence of ATP and Mg^{2+} ions (Figure 1A), but did not bind to ATP in the presence of EDTA (results not shown). We next mutated Lys[90] to a methionine or alanine residue. Lys[90] is predicted to lie in the β3 strand of TRB2, where it aligns with Lys[72] of PKA (Figure 1A) and its mutation has previously been shown to abolish ATP binding in unrelated kinases and pseudokinases [10,23]. As shown in Figure 2(A), K[90]M ($\Delta T_{m} = 1.59$ °C) and K[90]A ($\Delta T_{m} = 0.23$ °C), were both retarded in their ability to bind to ATP under these experimental conditions.

The ability of human TRB2 purified from *E. coli* to bind to ATP in the presence or absence of cofactors was next compared using a previously established TSA assay employing hydrophobic dye-binding [20,55]. In this procedure, ligand binding is evaluated based upon the thermal denaturation curves in the presence and absence of different cofactors using Sypro Orange (Supplementary Figure S3). In the presence of EDTA and ATP, both CASK and TRB2 exhibited demonstrable dose-dependent binding to ATP when compared with an EDTA alone control (Figure 2B). However, considerable stability (ΔT_{m} ~6 °C compared with a TRB buffer control) was imparted upon WT TRB2 in the presence of both 1 mM ATP and 2 mM EDTA (Figure 2C), demonstrating that it bound to ATP under these conditions, in marked contrast with Aurora A, which required ATP and Mg^{2+}-binding for stabilization (Figure 2D). Interestingly, the ΔT_{m} of ~2.93 °C for TRB2 in the presence of ATP and Mg^{2+} ions was considerably lower when compared with ATP and EDTA (ΔT_{m} ~6 °C), suggesting an inhibitory effect of cations on ATP binding. To evaluate the binding mode of ATP in TRB2, we next analysed the K[90]M and K[90]A point mutants using the Sypro Orange dye-binding procedure. In marked contrast with WT TRB2, the thermal stability of both K[90]M (Figure 2E) and K[90]A (Figure 2F) TRB2 mutants were not increased by ATP in combination with either EDTA or Mg^{2+} ions, in agreement with our findings from intrinsic fluorescence measurements (Figure 2A).

Recombinant human TRB2 (and TRB3) autophosphorylates in the absence of metal ions

Our finding that TRB2 (and CASK) could bind to low millimolar concentrations of ATP *in vitro* under two different sets of assay conditions raised the possibility that, despite their unusual catalytic make-up, they might both be catalytically competent to hydrolyse ATP. To investigate this possibility,
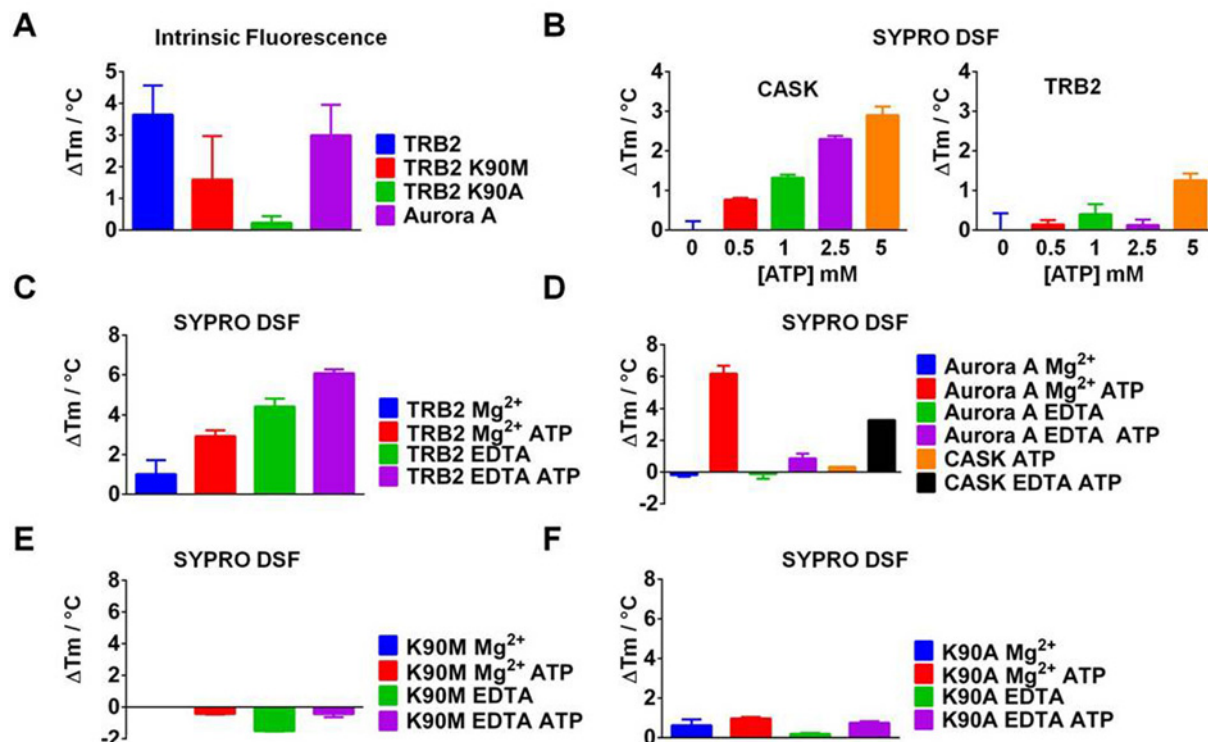
**Figure 2   TRB2 ATP binding detected by two complementary TSA approaches**

(**A**) Intrinsic fluorescence of 1 μg of purified recombinant TRB2 or the indicated K[90]M or K[90]A point mutants were analysed in the presence or absence of 1 mM unlabelled ATP in the presence of 2 mM EDTA in TRB buffer and compared with the canonical ATP-binding kinase Aurora A (purple bars), which was assayed in the presence of 10 mM Mg^{2+} ions but in the absence of EDTA. Proprietary Optim Avacta software was used to calculate average ΔT_{m} values ($\pm$ S.D.), which are normalized to buffer controls containing EDTA alone and are reported for triplicate assays from two independent experiments. Data were plotted using GraphPad Prism 6. (**B**) Sypro Orange fluorescence was detected using a standard TSA approach in a 96-well plate format using a real-time PCR machine and thermal ramping (0.3 °C/min over a range of 25 °C to 94 °C) in the presence or absence of the indicated concentrations of ATP + 2 mM EDTA using 5 μg of purified CASK (left panel) or TRB2 (right panel). Data were normalized to buffer controls containing 2 mM EDTA. (**C–F**) Analysis of TRB2 mutants. The ATP concentration was fixed at 1 mM and 10 mM MgCl$_2$ or 2 mM EDTA was added prior to analysis of the indicated protein. (**D**) CASK and Aurora A were employed as positive controls to confirm ATP binding under these assay condtions. (**C–F**) ΔT_{m} values are reported relative to a buffer blank control. Mean ΔT_{m} values ($\pm$ S.D.) are shown for each condition, determined from Boltzmann fitting of the data and plotted using GraphPad Prism 6 software. Note the effect of Lys^{90} mutations on the ability of TRB2 to bind ATP under all conditions tested.

we assayed TRB2 purified from *E. coli* alongside GST-tagged CASK, which is reported to autophosphorylate *in vitro* [9]. We performed *in vitro* kinase assays in the presence of EDTA (to chelate any contaminating metal ions) and in the absence of added divalent cations (Figure 3A). Like CASK, TRB2 autophosphorylation increased in a time-dependent manner under these conditions and the activity of TRB2 appeared to be similar or perhaps superior to that of CASK when compared by semi-quantitative autoradiography (Figure 3A). To quantify this activity at physiological pH, we assayed TRB2 and CASK side-by-side at pH 7.4 using a Tris-based buffer in which TRB2 could be stabilized for a limited period of time. We found that TRB2 possessed a $K_{\mathrm{m[ATP]}}$ value of 0.66 ± 0.35 mM, indicating higher ATP affinity when compared with CASK (1.64 ± 0.56 mM; Supplementary Figure S4A), although both exhibited much higher K_{m} values than the canonical kinase Aurora A in the presence of Mg^{2+}–ATP ($14.3 \pm 2.6 \mu$M), as expected. The stoichiometry of phosphate incorporation peaked for TRB2 at ∼0.01 mol of phosphate per mol of TRB2 and that of CASK was calculated to be maximal at ∼0.005 mol of phosphate per mol of protein, some 25-fold lower than previously reported for the GST-tagged CASK pseudokinase domain [9]. This very low incorporation, which is equivalent to phosphorylation of only 1 % of the total TRB2 protein present in

the assay, is one likely reason for our failure to map any site(s) of TRB2 autophosphorylation *in vitro*.

In contrast with our findings with TRB2 and CASK, the TRB-related pseudokinase SgK495, which contains a highly degraded pseudocatalytic site (Figure 1A) and the catalytically inactive pseudokinase STRADα, which binds, but does not hydrolyse, ATP [56] did not demonstrate the ability to autophosphorylate under these conditions (Figure 3A). As a control, D^{274}N Aurora A, in which the DFG motif was experimentally mutated to NFG, also lacked detectable activity when assayed side-by-side with TRB2 under the same conditions. As a positive control we confirmed that Aurora A, whose activity is known to be regulated by autophosphorylation [57,58], was active in the presence (but not the absence) of divalent metal ions (Figure 3B).

To confirm that TRB2 autophosphorylation was not the product of a contaminating bacterial kinase, we found that a K^{90}M mutation markedly reduced ATP binding (Figures 2A and 2E). We next showed that K^{90}M, but not K^{90}R, TRB2 was also defective in time-dependent autophosphorylation when relative activities were quantified (Figure 3C). CASK possesses the attributes of an Mg^{2+}-inhibited pseudokinase *in vitro* and so we analysed the effects of divalent ions on TRB2 activity, which we had shown reduced binding of ATP to TRB2 (Figure 2C). As shown in Figure 3(D), both TRB2 and the small amount of residual activity
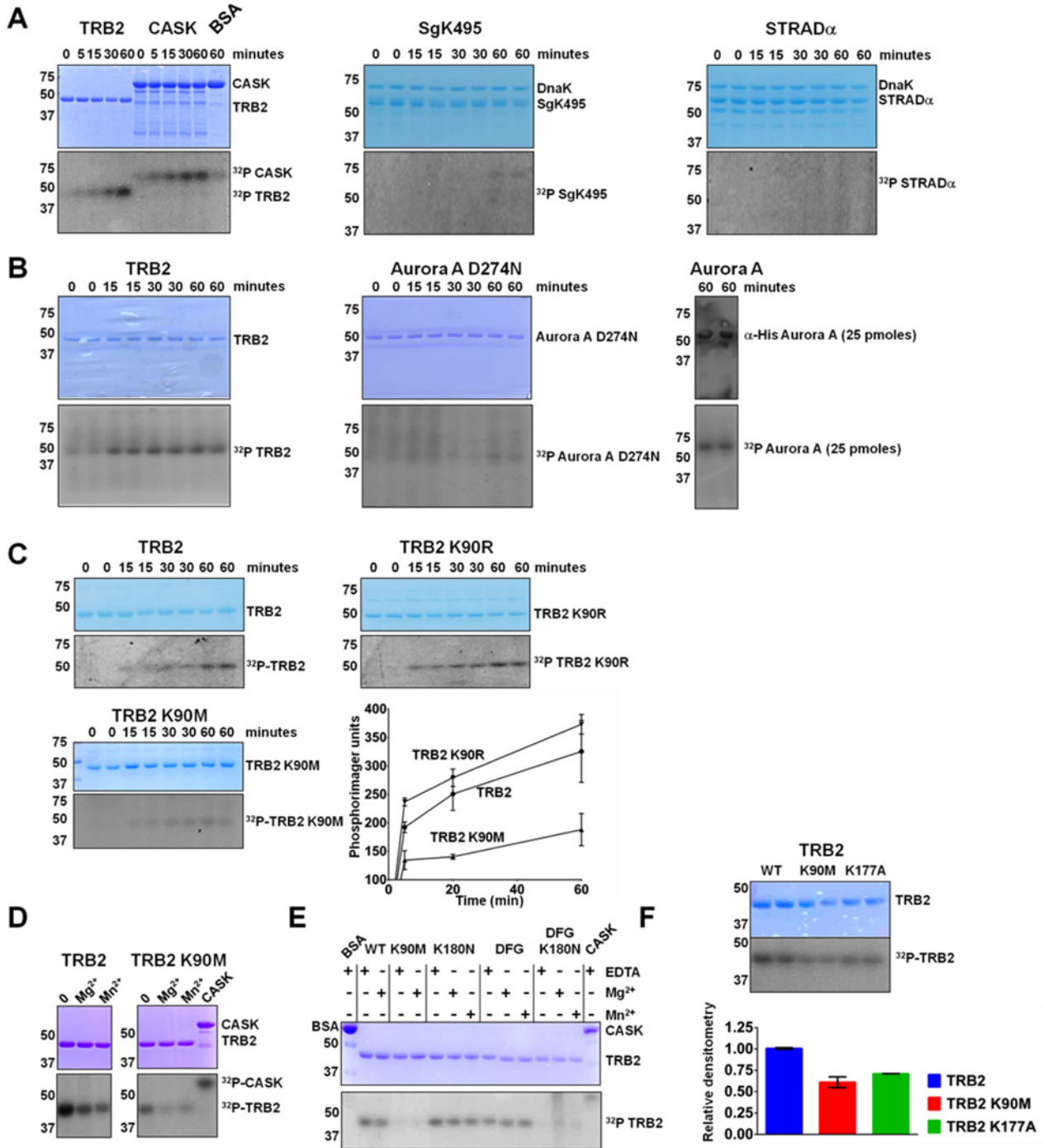
Figure 3   Analysis of pseudokinase autophosphorylation

(**A**) Bacterially produced and purified histidine-tagged TRB2 and GST–histidine–CASK (left panel), histidine-tagged SgK495 (which co-purifies with the heat-shock protein DnaK, middle panel) or histidine-tagged STRADα (also co-purifying with DnaK, right panel) were assayed in the presence of 1 mM [γ^{32}P]ATP (2.25 μCi) + 2 mM EDTA in TRB buffer (see the Experimental section) for the indicated times, prior to denaturation in SDS sample buffer and analysis by SDS/PAGE on 12 % gels. BSA was assayed for 60 min. Each protein (250 pmol) was assayed at each time point and phosphate incorporation was determined by autoradiography after Coomassie Blue staining and gel drying. All gels were processed side-by-side so that phosphorylation can be compared directly. Similar results were seen in multiple independent experiments. (**B**) Autophosphorylation of TRB2, Aurora A D^{274}N or Aurora A were evaluated in duplicate by autoradiography following SDS/PAGE analysis of *in vitro* kinase assays containing 250 pmol of TRB2 or Aurora A D^{274}N in the presence of EDTA or 25 pmol of Aurora A (right panel, quantified by Western blotting). All assays contained 1 mM [γ^{32}P]ATP (2.25 μCi) and 2 mM EDTA, except Aurora A, to which was added 10 mM Mg^{2+} ions in the absence of EDTA. (**C**) TRB2, TRB2 K^{90}R or TRB2 K^{90}M (250 pmol of each) was assayed in the presence of 2 mM EDTA and 1 mM [γ^{32}P]ATP (2.25 μCi) for the indicated time and autophosphorylation was quantified using a phosphorimager after SDS/PAGE. Duplicate readings were averaged and plotted on the graph, with error bars representing the S.D. from two independent experiments. (**D**) As in (**C**), except 250 pmol of TRB2 or K^{90}M TRB2 was assayed in the presence of 1 mM [γ^{32}P]ATP (2.25 μCi) in the presence of 10 mM MgCl$_2$ or 10 mM MnCl$_2$. CASK was included as a positive control. Phosphate incorporation was measured by autoradiography after the proteins were resolved by SDS/PAGE. (**E**) The TRB2 mutant K^{180}N, the triple mutant S^{195}D:L^{196}F:E^{197}G (DFG) or the quadruple mutant K^{180}N:S^{195}D:L^{196}F:E^{197}G (DFGK^{180}N) was assayed for 30 min in the presence of 2 mM EDTA, 10 mM MgCl$_2$ or 10 mM MnCl$_2$ as indicated. CASK was employed as a positive control and BSA was employed as negative control. (**F**) Analysis of TRB2 autophosphorylation alongside K^{177}A and K^{90}M point mutants. Data from two independent experiments were quantified by densitometric analysis using ImageJ software and presented in graphical format (bottom).

associated with the $K^{90}M$ TRB2 mutant, were inhibited by Mg^{2+} or Mn^{2+} ions when compared with an EDTA-alone control.

To extend these findings, we also compared the sensitivity of TRB2 to metal ions at physiological pH, using a Tris-based buffer in which TRB2 could be stabilized for a brief period of time. Interestingly, TRB2 was also catalytically active at pH 7.4 and autophosphorylation was inhibited by several divalent cations, including Mg^{2+}, Sr^{2+} and Cu^{2+} ions when compared with EDTA and Na^+ controls. In contrast, activity was largely unaffected by Ca^{2+} ions and preserved or increased in the presence of both Ni^{2+} and Co^{2+} divalent ions, which are known to interact with high affinity with His_6 motifs such as the N-terminal TRB2-affinity tag. Control experiments also confirmed dose-dependent inhibition by Mg^{2+} ions when compared with Na^+ and EDTA controls at pH 9.0 in a bicine-based buffer (Supplementary Figures S4B and S4C). It is known from previous work that replacing the equivalent lysine with the similarly charged basic arginine residue in canonical kinases such as Aurora A [57] or PKA [59] does not always abolish ATP binding. Therefore, to extend our findings to a second TRB-related pseudokinase, we found that TRB3, which was purified and assayed in an identical manner to TRB2, also autophosphorylated *in vitro* in the absence of metal ions at pH 9.0 in our standard TRB buffer (Supplementary Figure S4D). Consistently, this activity was also dependent on the conserved TRB3 lysine residue (Lys^{97}), since its mutation to methionine essentially abolished autophosphorylation.

As shown in Figure 1(A), TRB2 lacks all four canonical amino acids that form the asparagine and DFG metal-binding motif of most kinases. To attempt to reinstate metal-activated catalysis in TRB2, we introduced, either alone or in combination, the asparagine residue found in the catalytic loop of most kinases (TRB2 $K^{180}N$) or a triple 'DFG' motif ($S^{195}D$ $L^{196}F$ $E^{197}G$). As detailed in Figure 3(E), $K^{180}N$ and the triple DFG mutant all autophosphorylated in the absence of metals to a similar extent as WT TRB2, whereas the addition of 10 mM divalent cations did not enhance autophosphorylation, revealing a lack of any detectable effect on metal-stimulated TRB2 autophosphorylation caused by mutation. In contrast, the quadruple mutant was inactive (Figure 3E) and TSA confirmed that this was the result of this mutant being completely unfolded after purification (Supplementary Figure S3E). To enhance our analysis of the TRB2 ATP site, we also evaluated a $K^{177}A$ point mutant, similar to a mutation in TRB2 ($K^{177}R$) reported to prevent cellular transformation in cells [35]. This mutant exhibited consistently lower levels of activity than TRB2, which were comparable with those of the $K^{90}M$ mutant (Figure 3F). Finally, we investigated human TRB2 purified from eukaryotic Sf9 cells, where WT, $K^{90}M$ and quadruple-mutant TRB2 proteins were expressed at markedly different levels (Supplementary Figure S4E). Following IMAC purification and gel filtration, we confirmed that TRB2 also autophosphorylated weakly in the absence of metal ions, although this activity was much lower than human TRB2 isolated from bacteria. Unfortunately, the low expression of human TRB2 $K^{90}M$ and the instability of TRB2 $DFGK^{180}N$ after purification from Sf9 cells (Supplementary Figure S4E) prevented a side-by-side analysis of these three proteins.

## A screen for ligands that bind to TRB2 or 'analogue-sensitive' TRB2

Protein pseudokinases are a new class of drug targets [60] that make up a significant part of the 'untargeted' human kinome [61,62]. However, a paucity of well-validated targets and compounds has contributed to the lack of meaningful clinical targeting of pseudokinase domains [63]. The gatekeeper residue

is a key regulatory amino acid in kinases whose chemical nature and volume controls access to a drug-targetable hydrophobic pocket in kinases [64]. To evaluate TRB2 drug sensitivity using chemical genetics, two gatekeeper mutants ($F^{130}G$ and $F^{130}A$) were purified side-by-side with TRB2 (Supplementary Figure S5A) and denaturation profiles were initially analysed in the presence of a panel of 30 substituted PP compounds using Sypro Orange TSA in a 96-well format. Of this original panel, the chemical structures of seven related compounds that yielded the most readily interpretable TSA profiles with TRB2 are depicted in Figure 4(A). From this sub-panel, we found that only two compounds (termed A and F), exhibited little or no effect on TRB2, but led to marked stability of $F^{130}A$ (Figure 4A) and $F^{130}G$ TRB2 (results not shown), consistent with an interaction between the compound and the gatekeeper region in the enlarged TRB2 ATP site. Representative denaturation curves for these seven compounds are presented in Figures 4(B) and 4(C). Thermal stability was only consistent at high concentrations of inhibitor (250 μM), so to evaluate this interaction closely, we re-analysed compound B (dmB-PP1, a negative control) and compounds A (dClB-PP1) and F (bisPh-PP1) in three independent experiments. This analysis confirmed that dClB-PP1 and bisPh-PP1 led to stabilization of $F^{130}A$ TRB2 over the non-mutated TRB2 control (Figures 4D and 4E), with ΔT_m values of $\sim 15\,°C$, which is suggestive of a *bona fide* interaction. Interestingly, neither $F^{130}A$ nor $F^{130}G$ TRB2 mutants were able to autophosphorylate efficiently when compared with TRB2, suggesting that ATP (as opposed to selective compound) binding had been compromised by the mutations (Supplementary Figure S5B, quantified in C). This finding was supported by evaluation of the intrinsic fluorescence shift of $F^{130}A$ and $F^{130}G$ TRB2, which, like the $K^{90}M$ TRB2 mutant, exhibited significantly decreased ATP binding when compared with WT TRB2 (Supplementary Figure S5D). Finally, we employed intrinsic fluorescence to confirm specific binding of dClB-PP1 to both $F^{130}A$ and $F^{130}G$ TRB2, but not WT TRB2. Using this optimal assay procedure, we consistently measured a ΔT_m of 3–4 $°C$ in the presence of 250 μM dClB-PP1 (Supplementary Figure S5E).

DISCUSSION

The experimental findings reported in the present paper empower further studies aimed at TRB2 (and TRB3) analysis in biological settings. We initially discovered that recombinant TRB2 was highly unstable and rapidly denatured when isolated from either bacterial or Sf9 expression sources using our standard buffer conditions [44]. This problem, which may potentially be due to the absence of a stoichiometric binding partner or lack of a regulatory covalent modification, initially prevented in-depth TRB2 analysis, but this was resolved by stabilization of TRB2 at high concentrations in a bicine-based glycerol and saline mixture buffered at pH 9.0, although we were also able to assay TRB2 in a Tris-based buffer at pH 7.4 if purification and assay were performed very rapidly. Bicine is zwitterionic with a pK_a of 8.35 at 20 $°C$ [65] and has also been employed as a separation buffer for analysis of membrane proteins [66] and in the purification of PKA catalytic subunit mutants [67]. Our choice of bicine for the present study was influenced by a report evaluating conditions that promote protein stability *in vitro* [50]. Our new TRB stabilization procedure has allowed us to extend previous tentative observations, in which TRB2 was found to bind to ATP with a ΔT_m value below the (arbitrary) cut-off value [22] and go on to develop intrinsic and dye-binding fluorescence measurements for ATP binding that could be validated with
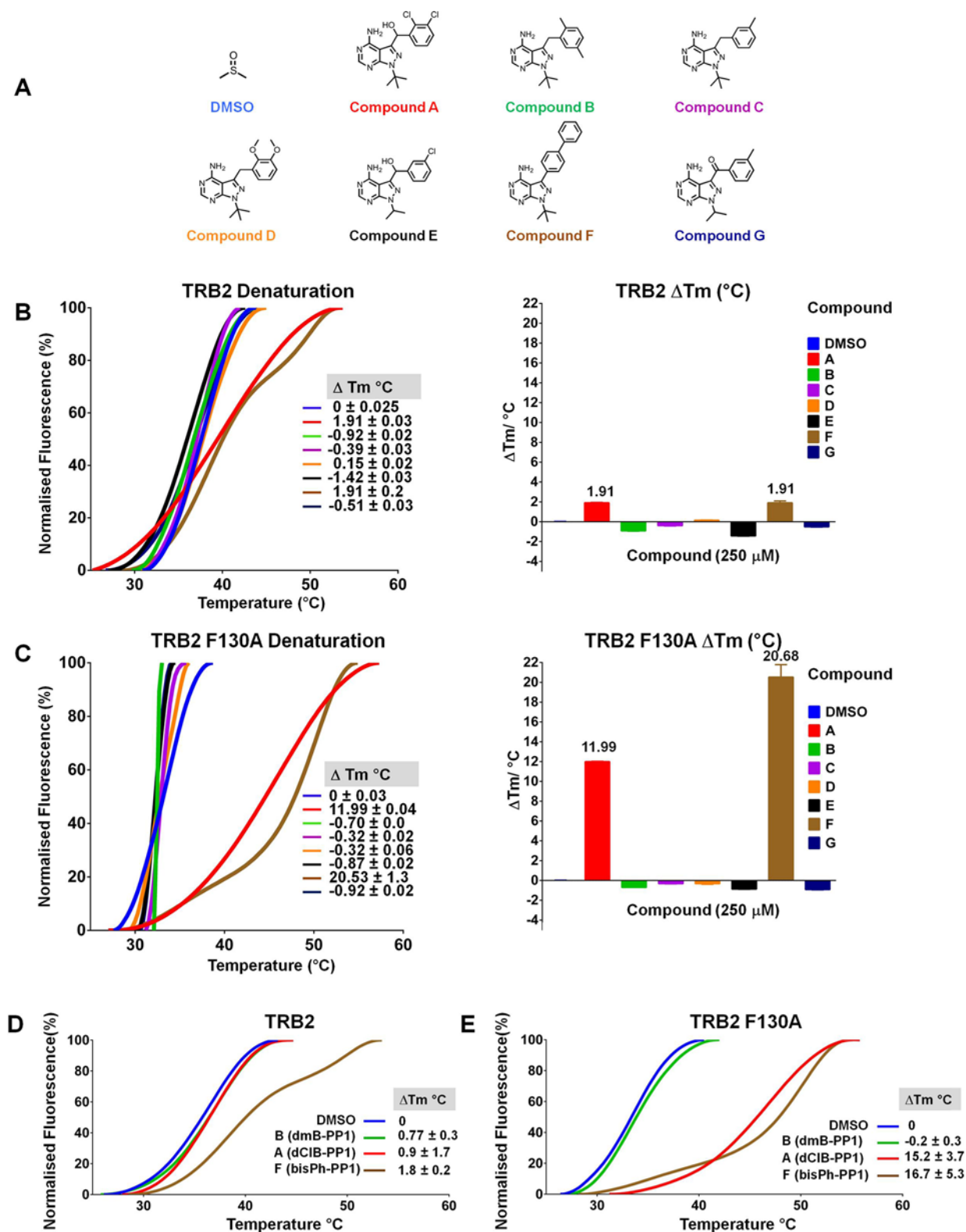
Figure 4   A focused small-molecule screen to evaluate TRB2 ligand binding

(**A**) Seven bulky 'bumped' PP1 analogues (termed A–G) were selected for further TSA analysis. (**B**) TSA assays containing 5 μg of purified TRB2 in TRB buffer were screened in triplicate in the presence of 250 μM of each compound and thermal stability at each temperature was normalized to 2.5 % (v/v) DMSO controls. A thermal ramping procedure (0.3 °C/min over a range of 25 °C to 94 °C) was employed to denature TRB2 and mean ΔT_m values ($\pm$ S.D.) are shown for each condition, determined from Boltzmann fitting of the data and plotted using GraphPad Prism 6 software. (**C**) Same as in (**B**), except a TRB2 F[130]A gatekeeper mutant was employed for the TSA screen, using the same panel of PP1 analogues. (**D** and **E**) The two hits from our secondary screen (compounds A and F) and one negative control (compound B) were taken forward and analysed in three independent experiments, each performed in duplicate and the data plotted after Boltzmann fitting using GraphPad Prism 6 software. ΔT_m values ($\pm$ S.D.) are presented for each compound.

binding-deficient point mutants. We report that TRB2 binds to ATP in the absence of divalent metal cations (controlled for experimentally by the addition of EDTA) and that binding (and autophosphorylation) is sensitive to relatively high (5–50 mM) concentrations of divalent cations *in vitro*. Our analysis suggests that cellular TRB2 nucleotide binding and any associated activity may be sensitive to fluxes of ATP and/or Mg^{2+} ions [68,69]. Total Mg^{2+} content, most of which is complexed to ATP and proteins, is estimated to be between 5 and 30 mM in human cells [70]. However, free levels of Mg^{2+} are thought to be very much lower (in the picomolar to nanomolar) range, although the function and spatial distribution of this difference remains enigmatic [71]. Our findings are supported by a side-by-side comparison with CASK, which exhibits 28 % identity in the pseudokinase domain to TRB2 and is already established to possess low levels of Mg^{2+}-inhibited phosphotransferase activity [9]. The observation that TRB2 autophosphorylates with a lower $K_{m[ATP]}$ value than CASK when assayed under identical assay conditions suggests that TRB2 may also possess intracellular substrates and signal through an ATP-regulated switching mechanism in cells, although further experiments will be required to confirm this theory.

Unfortunately, TRB1 (and to a certain extent TRB3) are highly challenging to purify and analyse, although we were able to confirm that, in contrast with SgK495 and STRADα, TRB3 possesses an intrinsic autophosphorylating activity that relies on a conserved lysine residue (Lys^{97}) localizing to the predicted β3 strand. Given the high level of identity between TRB2, TRB3 and TRB1 in the pseudokinase domain (Figure 1A), we also predict that TRB1 might exhibit weak ATP binding and retain low levels of enzymatic activity. The phosphotransferase activity associated with TRB2, which we calculate lies in the pmol/min/mg range (Supplementary Figure S4A), is very low when compared with canonical kinases assayed with optimized substrates, where nanomolar, or less commonly, μmol/min/mg rates of phosphorylation are known [57,59,72], but similar to those reported for the pseudokinases CASK [9] and HER3 [10]. Moreover, our biochemical analysis confirms that the activity is higher than the essentially undetectable levels of autophosphorylation artificially imparted on Aurora A when a $D^{274}N$ mutation is introduced in the DFG motif, which we assayed alongside TRB2 (Figure 2). It remains possible that TRB2 exhibits a different rate of catalysis in the presence of an appropriate substrate or regulatory subunit, although we were unable to demonstrate phosphorylation of classical non-specific kinase substrates such as myelin basic protein (MBP), mixed histones or α-casein *in vitro* or after concerted 'back-mutation', in an attempt to engineer high levels of activity, as has been previously achieved for CASK [24]. However, we speculate that the evolution and preservation of atypical TRB2 active site residues (Figure 5, see below) points to an important functional relevance that has been driven by the evolutionarily conserved roles of TRB pseudokinases, which uniquely regulate a select subset of ubiquitin E3 ligases in cells [26,31,33,35].

It has only recently been appreciated that protein kinases and pseudokinases possess a four order of magnitude range of affinities for Mg ATP, which can vary between sub-micromolar and millimolar levels when measured using a wide variety of *in vitro* and cellular measurements [15,16]. Like TRB2 and CASK, many documented canonical protein and lipid kinases have $K_{m[ATP]}$ values that are measured to lie at very high micromolar levels *in vitro*, with examples including validated catalytically active kinases such as CDK4–cyclin D, muscle-specific kinase (MuSK) and mammalian target of rapamycin (mTOR) that are thought to signal through ATP-dependent mechanisms in cells [15]. The values obtained in such

experiments are a function of the type of assay employed and the (pseudo)kinase source and, although ATP affinity is likely to vary depending on whether the kinase is pre-activated, bound to a regulatory protein or sourced from a non-physiological organism such as a bacterium, general trends (e.g. binding compared with non-binding, metal compared with metal–ATP complex) have already emerged among the pseudokinases [22]. In addition, the role of ligand binding has been appreciated to play a key role in cellular signalling of several kinases through ligand-bound conformational switches, which drive an allosteric effect independently of an ATP transferase activity in the kinase [73,74]. Such 'nucleotide-binding' mimicry is likely to be central to the way many (pseudo)kinases regulate signalling networks, especially those with low affinity for nucleotides such as TRB2.

A central finding from our study is that TRB2 ATP binding was detected most efficiently using intrinsic (internal) fluorescence measurements in combination with thermal unfolding. This approach is automated and can measure multiple parameters simultaneously in a 96-well format, including temperature-induced aggregation effects [54]. Dye-binding analysis has been used previously to analyse over 30 pseudokinases and is recognized as a useful general approach for ligand screening [20,75,76]. TSA reports the thermal stability of proteins, which usually increases when bound to a ligand in the ATP site. Although of general utility, this technique is not suitable for approximately 25 % of proteins evaluated in previous studies [20,50]. With this in mind, we believe that intrinsic fluorescence analysis is a useful advance for the analysis of pseudokinases and it is possible that pseudokinases such as TRB2, which is relatively unstable and particularly prone to denaturation and aggregation, are not ideally suited to dye-based reporters [22]. Other techniques involve monitoring fluorescent ATP probes such as 2′/3′-*O*-(*N*-methylanthraniloyl)-adenosine-5′-triphosphate (Mant-ATP) and TNP-ATP are reported to be much more susceptible to low signal-to-noise ratios that can lead to different findings when interpreting binding data [10,20,51–53]. Although we were able to obtain evidence for TNP-ATP binding by TRB2 that was competitive with ATP in the absence of Mg^{2+} ions (results not shown), we found that the data were somewhat subjective and that control proteins and buffer alone often gave very high fluorescence values. We therefore suggest that intrinsic and hydrophobic-dye binding might provide a useful comparative framework for the highly reproducible analysis of (pseudo)kinases in the future.

TRB2-specific variations in the active site and clues to a novel catalytic mechanism

Catalytic activity of TRB2 was observed in the absence of canonical active site residues, suggesting an unusual mechanism for ATP binding and phosphoryl-transfer that is dependent on Lys^{90}, which is equivalent to Lys^{72} of PKA [67]. Clues to such mechanisms can be obtained through analysis of TRB2 sequences and modelled structures. For example, close examination of TRB2 sequences from diverse organisms indicates a TRB-conserved glutamate residue at the DFG − 1 position and at the third residue of the canonical DFG triplet position (Figure 5; Supplementary Figure S1), which might potentially mimic the functions of the essential DFG aspartic acid residue. This hypothesis will need to be tested through further mutational studies that are outside the scope of the current study. However, our finding that mutation of SLE to DFG is unable to induce metal-dependent TRB2 activity *in vitro* and that a quadruple point mutant in which asparagine and DFG residues are introduced is inactive due to denaturation (Figure 3; Supplementary Figure 3E), suggests a fundamentally important role of these unique active site residues in the TRB
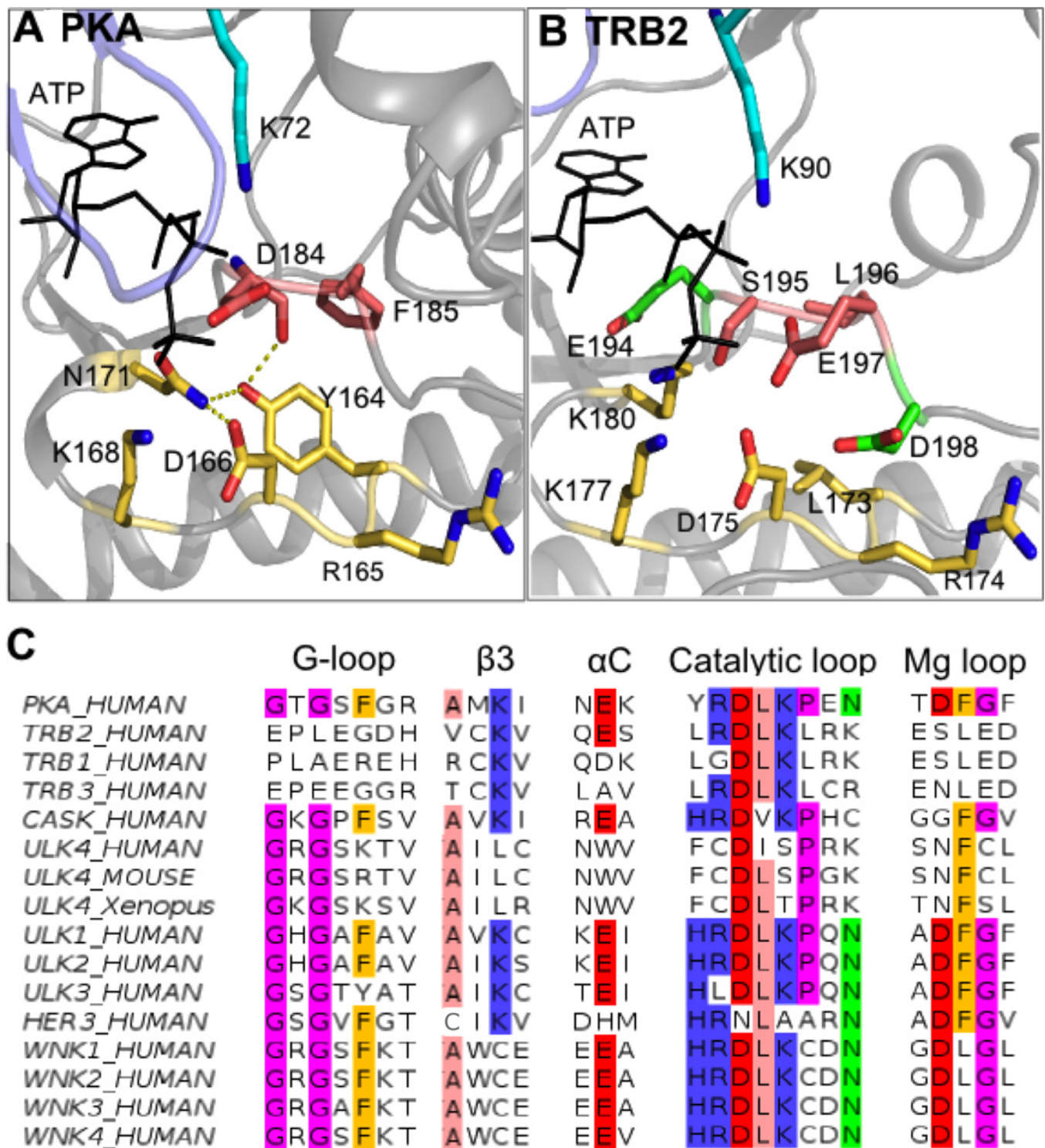
Figure 5   Comparison of the putative catalytic centre in TRB2 with PKA and selected pseudokinases

(**A**) Active site analysis of PKA showing the catalytically important residues. Amino acids around the ATP-binding site are shown in stick representation with colouring scheme as in Figure 1. (**B**) Active site of TRB2 based on the model presented in Figure 1 showing the conservation of some ATP-binding residues (e.g. Lys[90]) in β3 of the N-lobe, the putative catalytic base (Asp[175]) and Lys[177], which is required for optimal activity. The substitution of the DFG aspartic acid (Asp[184] in PKA) can potentially be rescued by the two charged residues shown in green (Glu[194] or Asp[198]). ATP is modelled based on alignment with PKA. (**C**) Multiple numbered alignment of PKA, human TRB1-3, CASK, ULK4 (human, mouse and frog), ULK1-3, HER3 and WNK1-4, which were formatted in JalView. Note the presence of conserved lysine and arginine residues in the ULK4 pseudokinase G-loop that are absent from ULK1-3 kinase homologues and similar disposition of charged lysine residue in all four WNK proteins. The plethora of cysteine residues in the β3 strand of these pseudokinases might be targeted with appropriate irreversible ligands.

pseudokinase homologues. Comparison of active site geometry in PKA and the modelled TRB2 structure indicates additional variations in the active site that support an unusual mechanism of action. For example, the conserved histidine/tyrosine within the [H/Y]RD motif of PKA is replaced by a leucine in TRB2. This variation is predicted to disrupt the canonical hydrogen bonding interactions between the [H/Y]RD histidine side chain and the DFG backbone, thereby promoting a unique DFG motif backbone geometry (compare Figures 5A and 5B).

Kinome-wide analysis indicates that the ESLE motif is unique to TRB and is preserved from flies to vertebrates (Figure 5C). Interestingly, the small-molecule (non-protein) kinase choline kinase also contain a negatively charged amino acid at this position, which has been proposed to play a role in the product release cycle of this class of enzyme. Moreover, Lys^{180} at the end of the putative catalytic loop (Figure 5B) is also observed in the pseudokinase ULK4 (Unc-51-related kinase-4), which is closely related to the autophagy–related 1 (Atg1) tumour-suppressor ULK1, a central regulator of autophagy as part of the mTOR complex [77,78]. Interestingly, we ascertained that mutation of Lys^{180} to asparagine did not diminish TRB2 activity, whereas mutation of Lys^{177} to alanine did (Figure 3F), supporting an interesting observation in human cells, where mutation at Lys^{177} markedly reduced cloning efficiency of cells overexpressing human TRB2 [35]. ULK4 exhibits ∼24 % identity with TRB2 and also lacks the canonical DFG aspartic acid and HRD histidine residues (Figure 5C). Thus, although the specific function and mechanism of action of ULK4 is not known, we speculate that an unusual phosphoryl-transfer mechanism similar to TRB2 might also impart some catalytic potential towards ULK4, which has recently been demonstrated (somewhat surprisingly) to bind to ATP in the absence of metal ions *in vitro*, despite lacking either canonical VAIK, HRD or DFG motifs [22]. In ULK4, the canonical β3 lysine residue (Figure 1A) is changed to a leucine, but is conserved as a lysine in the canonical kinases ULK1–3 (Figure 5C). Our finding that TRB2 possesses low-affinity ATP binding and autophosphorylation in the context of an unusual active site might help reconcile this difference and we speculate that the lack of an essential ATP-binding basic residue in the ULK4 β3 strand might be rescued by the lysine or arginine residue that are found uniquely in the glycine-rich loop of ULK4. A structurally and mechanistically validated precedent for such a replacement already exists among the with no lysine (WNK) kinases [79], of which all utilize a similar compensatory mechanism for ATP binding (Figure 5C) that has evolved to permit an intracellular ion-sensing function in this region of WNK1 [80]. The recent finding that ULK4 is expressed in brain and implicated as a schizophrenia-susceptibility gene [81] and is a risk allele for multiple myeloma in humans [82] suggests that it is worthy of closer investigation. Indeed, deletion of ULK4 in mice is associated with congenital hydrocephalus [83], whereas knockdown influences several canonical MAPK (mitogen-activated protein kinase) signalling pathways in human cells, so the investigation of ULK4 signalling potential in these contexts [81] will be of particular interest.

The absence of a DFG motif in TRB2 suggests that the canonical DFG in and out switching mechanism of 'stabilization' of the active and inactive conformations found in many other kinases might be compromised. However, it has recently been appreciated that amino acids adjacent to the DFG motif, including the DFG −1 residue (conserved as glutamic acid in TRB pseudokinases; Figure 5C) or the DFG +1 residue (conserved as aspartic acid in TRB pseudokinases; Figure 5C) are also critical for several features of active kinase conformations, catalysis or sensitivity to clinical kinase inhibitors [93]. For example, in both size and chemical nature, the DFG −1 residue and the gatekeeper residue impart structural restrictions on how small molecules drive the active and inactive conformation of several model kinases [84]. Furthermore, the nature of the DFG +1 amino acid has also recently been reported to influence choice of substrate phosphorylation, with mutatable programming of kinases for serine compared with threonine specificity of phosphorylation in a cellular context [85]. Furthermore, a common cancer driver mutation in the EGFR DFG +1 residue ($L^{858}R$) markedly sensitizes this tyrosine kinase to the drug gefitinib [86] and that of the serine/threonine kinase Aurora A to a related quinazoline inhibitor [87]. The unusual and, to our knowledge, unique endowment of charged residues in the non-canonical setting of the TRB-active site at the equivalent positions to these residues might reflect a conserved mechanistic link that harmonizes signalling potential to the appropriate phenotype. However, these residues are also likely to be important for dictating sensitivity to small molecule inhibitors. It will be interesting to observe whether ligands designed to target TRB2 can exploit these conserved features and whether such compounds exert (pseudo)kinase specificity, marking them out as useful chemical biology probes for TRB2 analysis.

Chemical genetic analysis reveals a ligand-targetable ATP-binding site in TRB2

The majority of CAMK and CMGC (cyclin–dependent kinase, mitogen-activated protein kinase, glycogen synthase kinase, cyclin-dependent kinase-like kinase) families, which are the two most closely related kinase families to the TRB pseudokinases, contain a phenylalanine gatekeeper residue whose mutation often preserves catalytic potential [88,89]. TRB2 possesses a phenylalanine gatekeeper (Supplementary Figure S5A) and we found that bacterially expressed TRB2 $F^{130}A$ or $F^{130}G$ mutants exhibited very low levels of autophosphorylation and ATP binding. However, since this approach is already known to alter the phosphotransferase activity of many other kinases, due to an involvement of the gatekeeper residue in stabilizing the C-spine in the active kinase conformation [90], we suggest that these precedents add further credence to our finding that WT TRB2 can adopt an active conformation and autophosphorylate at low levels (Figure 3). The ability of TRB2 to bind to ATP in a manner reliant on Lys^{90} (Figures 2 and 3) raised the possibility of discovering novel ligands that also interact with the TRB2 catalytic site. Targeting a specific protein kinase with a kinase inhibitor is inherently difficult because of the high degree of conservation shared between all kinase domains in the human kinome and the promiscuity of small molecules developed to target them [91,92]. Within the kinome, the gatekeeper amino acid occludes the binding of bulky kinase inhibitor analogues (e.g. PP1 analogues), since they cannot access a hydrophobic cavity located within the ATP-binding pocket. Most clinically approved kinase inhibitors target kinases with a small (threonine) gatekeeper residue, although only ∼20 % of the human kinome have evolved a serine/threonine amino acid in this position [93]. No human kinase possesses the smallest amino acid side-chains (glycine or alanine) and following mutation to either of these residues, the enlarged ATP-binding pockets of such AS gatekeeper kinases now possess the ability to specifically interact with bulky kinase inhibitor analogues, which have the enormous advantage of being unable to target the vast majority of kinase ATP-binding sites in endogenous protein kinases [94]. We found that two such compounds, dClB-PP1 and bisPh-PP1, bound specifically to TRB2 when an $F^{130}A$ or $F^{130}G$ gatekeeper was present. Although a

weak binding to the WT TRB2 was evident, the increase in thermal stability of TRB2 $F^{130}A$ suggests a markedly enhanced interaction with these two compounds. It will be important to analyse the SAR (structure activity relationship) of additional compounds *in vitro*, including the interesting ability of TRB2 $F^{130}A$ to discriminate between two very similar mono- and di-chloro PP1 analogues (compounds A and E; Figure 4A). In the future, we might also extend our initial findings into human cells to evaluate effects of small molecules on TRB2-regulated signalling pathways. A key outcome of the present work is confirmation that the TRB2 ATP site can be targeted with specific small molecule ligands. Given the relatively low TRB2 affinity for ATP and the highly unusual set of amino acids that are present in all TRB pseudokinases (Figure 5), it is likely that atypical classes of chemical ligands will need to be designed in order for a high-affinity TRB2 interaction to be engineered. In this regard, covalent inhibitors of protein kinases have recently been recognized as useful tools and clinical compounds for the significant number of kinome members containing a cysteine residue [90,95,96]. We note the presence of a cysteine residue in the $\beta3$ lysine motif of TRB, ULK4, WNK and HER3 pseudokinases, targeting of which might be critical to impart stability and specificity on a designer small molecule ligand (Figure 5C). Such a covalent strategy has recently come to fruition for the pseudokinase HER3 [97], with the development of electrophilic compounds that covalently link to the cysteine residue lying two amino acids N-terminal to the catalytic $\beta3$ lysine residue (Figure 5C). The advantage of this type of compound is the opportunity for specificity in the ATP site and the ability for high-precision chemical genetic experiments to be performed [95]. We believe that targeting of the previously overlooked TRB2 Cys^{89} equivalent in pseudokinases (Figure 5C) might also be a useful opportunity for novel compound development in the future.

Significance

The described functions of TRB can be separated into two non-mutually exclusive classes: putative scaffolding roles for canonical kinase modules (e.g. TRB2 and TRB3 in MAPK and Akt (Ak strain transforming/v-Akt murine thymoma viral oncogene) signalling respectively [25,36,98–100]) or as regulators of transcription factor ubiquitination, driven through engagement of the TRB C-terminal motif that targets ubiquitin E3 ligases such as COP1 (constitutive photomorphogenic protein 1) and TRIM21 (tripartite motif-containing protein 21) [33,101]. A role for the TRB2 pseudokinase domain, which we speculate functions in vertebrates as a modulator of TRB-mediated ubiquitination events, is inferred directly from the conserved primary structure of the TRB pseudokinases, which have evolved to position the canonical E3 ligase-binding motif C-terminal to the pseudokinase domain (Supplementary Figure S1). Indeed, TRB-driven transcription factor ubiquitination and proteasome-mediated destruction is conserved from flies to humans [26,35] and cellular analysis of the role of interfering mutations within the TRB2 kinase domain such as $K^{90}M$ or $K^{90}A$, which suppress ATP binding and autophosphorylation *in vitro*, are likely to be revealing. In order to reveal specific cellular functions of nucleotide binding, catalysis or a regulated conformational change that might resemble ATP binding [21], we are in the process of generating knockin cells using CRISPR–Cas9 (clustered regularly interspaced short palindromic repeats–CRISPR-associated protein 9) endonuclease technology [102] to study TRB2 signalling in a controlled genetic background. TRB2 mutants will also be critical to confirm whether small

molecule compounds that bind to the TRB2 pseudokinase site mimic effects of ATP binding (perhaps acting like conventional pharmacological agonists) or whether they prevent ATP binding and therefore ameliorate TRB2 effects on downstream signalling (fulfilling the role of pharmacological antagonists). As pointed out for ligands that bind to HER3, such binding-mode discrimination is important if compounds are to be exploited for effective blockade of disease-associated signalling outcomes rather than to promote them [97,103–105]. In the context of cancer, where TRB2 overexpression is clearly linked to proliferation and disease through regulation of multiple different signalling pathways [35,101,106,107], a judicious selection of compound classes with the latter phenotypic effects should be sought out for initial evaluation. Indeed, our analysis of TRB pseudokinases shows that they are differentially mutated in human malignancies, with conserved mutations mapping to several unknown regulatory sites on the TRB pseudocatalytic domain (Supplementary Figure S6). Interestingly, these mutations cluster around the predicted G and H helices, which are thought to be involved in stabilization of the ATP site and alignment of the catalytic spine in model kinases [47]. Of particular interest in TRB2 is amino acid Asp^{211}, which lies at the equivalent position of Thr^{197} in the activation loop of PKA (Figure 1A). We identified two independent cancer samples where this residue is mutated to an uncharged asparagine side chain and exploring the effects of this significant substitution will also be of interest in cellular contexts, where small molecule TRB2 targeting is likely to yield interesting biological effects.

REFERENCES

1 Zeqiraj, E. and van Aalten, D.M. (2010) Pseudokinases-remnants of evolution or key allosteric regulators? Curr. Opin. Struct. Biol. **20**, 772–781 CrossRef PubMed

2 Eyers, P.A. and Murphy, J.M. (2013) Dawn of the dead: protein pseudokinases signal new adventures in cell biology. Biochem. Soc. Trans. **41**, 969–974 CrossRef PubMed

3 Manning, G., Whyte, D.B., Martinez, R., Hunter, T. and Sudarsanam, S. (2002) The protein kinase complement of the human genome. Science **298**, 1912–1934 CrossRef PubMed

4 Kannan, N., Taylor, S.S., Zhai, Y., Venter, J.C. and Manning, G. (2007) Structural and functional diversity of the microbial kinome. PLoS Biol. **5**, e17 CrossRef PubMed

5 Manning, G., Reiner, D.S., Lauwaet, T., Dacre, M., Smith, A., Zhai, Y., Svard, S. and Gillin, F.D. (2011) The minimal kinome of *Giardia lamblia* illuminates early kinase evolution and unique parasite biology. Genome Biol. **12**, R66 CrossRef PubMed

6 Mendrola, J.M., Shi, F., Park, J.H. and Lemmon, M.A. (2013) Receptor tyrosine kinases with intracellular pseudokinase domains. Biochem. Soc. Trans. **41**, 1029–1036 CrossRef PubMed

7   Taylor, S.S., Shaw, A., Hu, J., Meharena, H.S. and Kornev, A. (2013) Pseudokinases from a structural perspective. Biochem. Soc. Trans. **41**, 981–986 CrossRef PubMed

8   Reiterer, V., Eyers, P.A. and Farhan, H. (2014) Day of the dead: pseudokinases and pseudophosphatases in physiology and disease. Trends Cell Biol. **24**, 489–505 CrossRef PubMed

9   Mukherjee, K., Sharma, M., Urlaub, H., Bourenkov, G.P., Jahn, R., Sudhof, T.C. and Wahl, M.C. (2008) CASK Functions as a Mg^{2+}-independent neurexin kinase. Cell **133**, 328–339 CrossRef PubMed

10 Shi, F., Telesco, S.E., Liu, Y., Radhakrishnan, R. and Lemmon, M.A. (2010) ErbB3/HER3 intracellular domain is competent to bind ATP and catalyze autophosphorylation. Proc. Natl. Acad. Sci. U.S.A. **107**, 7692–7697 CrossRef PubMed

11 Ungureanu, D., Wu, J., Pekkala, T., Niranjan, Y., Young, C., Jensen, O.N., Xu, C.F., Neubert, T.A., Skoda, R.C., Hubbard, S.R. and Silvennoinen, O. (2011) The pseudokinase domain of JAK2 is a dual-specificity protein kinase that negatively regulates cytokine signaling. Nat. Struct. Mol. Biol. **18**, 971–U921 CrossRef PubMed

12 Brennan, D.F., Dar, A.C., Hertz, N.T., Chao, W.C., Burlingame, A.L., Shokat, K.M. and Barford, D. (2011) A Raf-induced allosteric transition of KSR stimulates phosphorylation of MEK. Nature **472**, 366–369 CrossRef PubMed

13 Kannan, N. and Taylor, S.S. (2008) Rethinking pseudokinases. Cell **133**, 204–205 CrossRef PubMed

14 Traut, T.W. (1994) Physiological concentrations of purines and pyrimidines. Mol. Cell. Biochem. **140**, 1–22 CrossRef PubMed

15 Knight, Z.A. and Shokat, K.M. (2005) Features of selective kinase inhibitors. Chem. Biol. **12**, 621–637 CrossRef PubMed

16 Becher, I., Savitski, M.M., Savitski, M.F., Hopf, C., Bantscheff, M. and Drewes, G. (2013) Affinity profiling of the cellular kinome for the nucleotide cofactors ATP, ADP, and GTP. ACS. Chem. Biol. **8**, 599–607 CrossRef PubMed

17 Talevich, E. and Kannan, N. (2013) Structural and evolutionary adaptation of rhoptry kinases and pseudokinases, a family of coccidian virulence factors. BMC Evol. Biol. **13**, 117 CrossRef PubMed

18 Kornev, A.P. and Taylor, S.S. (2009) Pseudokinases: functional insights gleaned from structure. Structure **17**, 5–7 CrossRef PubMed

19 Scheeff, E.D., Eswaran, J., Bunkoczi, G., Knapp, S. and Manning, G. (2009) Structure of the pseudokinase VRK3 reveals a degraded catalytic site, a highly conserved kinase fold, and a putative regulatory binding site. Structure **17**, 128–138 CrossRef PubMed

20 Lucet, I.S., Babon, J.J. and Murphy, J.M. (2013) Techniques to examine nucleotide binding by pseudokinases. Biochem. Soc. Trans. **41**, 975–980 CrossRef PubMed

21 Hu, J., Yu, H., Kornev, A.P., Zhao, J., Filbert, E.L., Taylor, S.S. and Shaw, A.S. (2011) Mutation that blocks ATP binding creates a pseudokinase stabilizing the scaffolding function of kinase suppressor of Ras, CRAF and BRAF. Proc. Natl. Acad. Sci. U.S.A. **108**, 6067–6072 CrossRef PubMed

22 Murphy, J.M., Zhang, Q., Young, S.N., Reese, M.L., Bailey, F.P., Eyers, P.A., Ungureanu, D., Hammaren, H., Silvennoinen, O., Varghese, L.N. et al. (2014) A robust methodology to subclassify pseudokinases based on their nucleotide-binding properties. Biochem. J. **457**, 323–334 CrossRef PubMed

23 Murphy, J.M., Lucet, I.S., Hildebrand, J.M., Tanzer, M.C., Young, S.N., Sharma, P., Lessene, G., Alexander, W.S., Babon, J.J., Silke, J. and Czabotar, P.E. (2014) Insights into the evolution of divergent nucleotide-binding mechanisms among pseudokinases revealed by crystal structures of human and mouse MLKL. Biochem. J. **457**, 369–377 CrossRef PubMed

24 Mukherjee, K., Sharma, M., Jahn, R., Wahl, M.C. and Sudhof, T.C. (2010) Evolution of CASK into a Mg^{2+}-sensitive kinase. Sci. Signal. **3**, ra33 PubMed

25 Kiss-Toth, E., Bagstaff, S.M., Sung, H.Y., Jozsa, V., Dempsey, C., Caunt, J.C., Oxley, K.M., Wyllie, D.H., Polgar, T., Harte, M. et al. (2004) Human tribbles, a protein family controlling mitogen-activated protein kinase cascades. J. Biol. Chem. **279**, 42703–42708 CrossRef PubMed

26 Masoner, V., Das, R., Pence, L., Anand, G., LaFerriere, H., Zars, T., Bouyain, S. and Dobens, L.L. (2013) The kinase domain of *Drosophila* tribbles is required for turnover of fly C/EBP during cell migration. Dev. Biol. **375**, 33–44 CrossRef PubMed

27 Seher, T.C. and Leptin, M. (2000) Tribbles, a cell-cycle brake that coordinates proliferation and morphogenesis during *Drosophila* gastrulation. Curr. Biol. **10**, 623–629 CrossRef PubMed

28 Mata, J., Curado, S., Ephrussi, A. and Rorth, P. (2000) Tribbles coordinates mitosis and morphogenesis in *Drosophila* by regulating string/CDC25 proteolysis. Cell **101**, 511–522 CrossRef PubMed

29 Grosshans, J. and Wieschaus, E. (2000) A genetic link between morphogenesis and cell division during formation of the ventral furrow in *Drosophila*. Cell **101**, 523–531 CrossRef PubMed

30 Das, R., Sebo, Z., Pence, L. and Dobens, L.L. (2014) *Drosophila* tribbles antagonizes insulin signaling-mediated growth and metabolism via interactions with Akt kinase. PLoS One **9**, e109530 CrossRef PubMed

31 Keeshan, K., He, Y.P., Wouters, B.J., Shestova, O., Xu, L.W., Sai, H., Rodriguez, C.G., Maillard, I., Tobias, J.W., Valk, P. et al. (2006) Tribbles homolog 2 (Trib2) inactivates C/EBPalpha and causes acute myelogenous leukemia. Cancer Cell **10**, 401–411 CrossRef PubMed

32 Lohan, F. and Keeshan, K. (2013) The functionally diverse roles of tribbles. Biochem. Soc. Trans. **41**, 1096–1100 CrossRef PubMed

33 Dedhia, P.H., Keeshan, K., Uljon, S., Xu, L.W., Vega, M.E., Shestova, O., Zaks-Zilberman, M., Romany, C., Blacklow, S.C. and Pear, W.S. (2010) Differential ability of tribbles family members to promote degradation of C/EBP alpha and induce acute myelogenous leukemia. Blood **116**, 1321–1328 CrossRef PubMed

34 Rishi, L., Hannon, M., Salome, M., Hasemann, M., Frank, A.K., Campos, J., Timoney, J., O'Connor, C., Cahill, M.R., Porse, B. and Keeshan, K. (2014) Regulation of Trib2 by an E2F1-C/EBPalpha feedback loop in AML cell proliferation. Blood **123**, 2389–2400 CrossRef PubMed

35 Keeshan, K., Bailis, W., Dedhia, P.H., Vega, M.E., Shestova, O., Xu, L., Toscano, K., Uljon, S.N., Blacklow, S.C. and Pear, W.S. (2010) Transformation by tribbles homolog 2 (Trib2) requires both the Trib2 kinase domain and COP1 binding. Blood **116**, 4948–4957 CrossRef PubMed

36 Izrailit, J., Berman, H.K., Datti, A., Wrana, J.L. and Reedijk, M. (2013) High throughput kinase inhibitor screens reveal TRB3 and MAPK-ERK/TGFβ pathways as fundamental Notch regulators in breast cancer. Proc. Natl. Acad. Sci. U.S.A. **110**, 1714–1719 CrossRef PubMed

37 Wennemers, M., Bussink, J., Scheijen, B., Nagtegaal, I.D., van Laarhoven, H.W., Raleigh, J.A., Varia, M.A., Heuvel, J.J., Rouschop, K.M., Sweep, F.C. and Span, P.N. (2011) Tribbles homolog 3 denotes a poor prognosis in breast cancer and is involved in hypoxia response. Breast Cancer Res. **13**, R82 CrossRef PubMed

38 Hanks, S.K. and Hunter, T. (1995) Protein kinases 6. The eukaryotic protein kinase superfamily: kinase (catalytic) domain structure and classification. FASEB J. **9**, 576–596 PubMed

39 Troshin, P.V., Procter, J.B. and Barton, G.J. (2011) Java bioinformatics analysis web services for multiple sequence alignment–JABAWS:MSA. Bioinformatics **27**, 2001–2002 CrossRef PubMed

40 Forbes, S.A., Bhamra, G., Bamford, S., Dawson, E., Kok, C., Clements, J., Menzies, A., Teague, J.W., Futreal, P.A. and Stratton, M.R. (2008) The catalogue of somatic mutations in cancer (COSMIC). Curr. Protoc. Hum. Genet. **Chapter 10**, Unit 10. 11 PubMed

41 Gosal, G., Kochut, K.J. and Kannan, N. (2011) ProKinO: an ontology for integrative analysis of protein kinases in cancer. PLoS One **6**, e28782 CrossRef PubMed

42 McSkimming, D.I., Dastgheib, S., Talevich, E., Narayanan, A., Katiyar, S., Taylor, S.S., Kochut, K. and Kannan, N. (2015) ProKinO: a unified resource for mining the cancer kinome. Hum. Mutat. **36**, 175–186 PubMed

43 Talevich, E. and Kannan, N. (2013) Structural and evolutionary adaptation of rhoptry kinases and pseudokinases, a family of coccidian virulence factors. BMC Evol. Biol. **13**, 117 CrossRef PubMed

44 Scutt, P.J., Chu, M.L., Sloane, D.A., Cherry, M., Bignell, C.R., Williams, D.H. and Eyers, P.A. (2009) Discovery and exploitation of inhibitor-resistant aurora and polo kinase mutants for the analysis of mitotic networks. J. Biol. Chem. **284**, 15880–15893 CrossRef PubMed

45 Zhang, C., Lopez, M.S., Dar, A.C., Ladow, E., Finkbeiner, S., Yun, C.H., Eck, M.J. and Shokat, K.M. (2013) Structure-guided inhibitor design expands the scope of analog-sensitive kinase technology. ACS Chem. Biol. **8**, 1931–1938 CrossRef PubMed

46 Cho, Y.S., Yoo, J., Park, S. and Cho, H.S. (2014) The structures of the kinase domain and UBA domain of MPK38 suggest the activation mechanism for kinase activity. Acta Crystallogr. D Biol. Crystallogr. **70**, 514–521 CrossRef PubMed

47 Kornev, A.P., Taylor, S.S. and Ten Eyck, L.F. (2008) A helix scaffold for the assembly of active protein kinases. Proc. Natl. Acad. Sci. U.S.A. **105**, 14377–14382 CrossRef PubMed

48 Kornev, A.P., Haste, N.M., Taylor, S.S. and Eyck, L.F. (2006) Surface comparison of active and inactive protein kinases identifies a conserved activation mechanism. Proc. Natl. Acad. Sci. U.S.A. **103**, 17783–17788 CrossRef PubMed

49 Johnson, L.N. and Lewis, R.J. (2001) Structural basis for control by phosphorylation. Chem. Rev. **101**, 2209–2242 CrossRef PubMed

50 Vedadi, M., Niesen, F.H., Allali-Hassani, A., Fedorov, O.Y., Finerty, Jr, P.J., Wasney, G.A., Yeung, R., Arrowsmith, C., Ball, L.J. et al. (2006) Chemical screening methods to identify ligands that promote protein stability, protein crystallization, and structure determination. Proc. Natl. Acad. Sci. U.S.A. **103**, 15835–15840 CrossRef PubMed

51 Sierke, S.L., Cheng, K., Kim, H.H. and Koland, J.G. (1997) Biochemical characterization of the protein tyrosine kinase homology domain of the ErbB3 (HER3) receptor protein. Biochem. J. **322**, 757–763 PubMed

52 Guy, P.M., Platko, J.V., Cantley, L.C., Cerione, R.A. and Carraway, III, K.L. (1994) Insect cell-expressed p180erbB3 possesses an impaired tyrosine kinase activity. Proc. Natl. Acad. Sci. U.S.A. **91**, 8132–8136 CrossRef PubMed

53 Cheng, K. and Koland, J.G. (1996) Nucleotide binding by the epidermal growth factor receptor protein-tyrosine kinase. Trinitrophenyl-ATP as a spectroscopic probe. J. Biol. Chem. **271**, 311–318 CrossRef PubMed

54 Gaudet, M., Remtulla, N., Jackson, S.E., Main, E.R., Bracewell, D.G., Aeppli, G. and Dalby, P.A. (2010) Protein denaturation and protein:drugs interactions from intrinsic protein fluorescence measurements at the nanolitre scale. Protein Sci. **19**, 1544–1554 CrossRef PubMed

55 Niesen, F.H., Berglund, H. and Vedadi, M. (2007) The use of differential scanning fluorimetry to detect ligand interactions that promote protein stability. Nat. Protoc. **2**, 2212–2221 CrossRef PubMed

56 Zeqiraj, E., Filippi, B.M., Goldie, S., Navratilova, I., Boudeau, J., Deak, M., Alessi, D.R. and van Aalten, D.M. (2009) ATP and MO25alpha regulate the conformational state of the STRADalpha pseudokinase and activation of the LKB1 tumour suppressor. PLoS Biol. **7**, e1000126 CrossRef PubMed

57 Haydon, C.E., Eyers, P.A., Aveline-Wolf, L.D., Resing, K.A., Maller, J.L. and Ahn, N.G. (2003) Identification of novel phosphorylation sites on *Xenopus laevis* Aurora A and analysis of phosphopeptide enrichment by immobilized metal-affinity chromatography. Mol. Cell. Proteomics **2**, 1055–1067 CrossRef PubMed

58 Eyers, P.A. and Maller, J.L. (2004) Regulation of *Xenopus* Aurora A activation by TPX2. J. Biol. Chem. **279**, 9008–9015 CrossRef PubMed

59 Gibbs, C.S. and Zoller, M.J. (1991) Rational scanning mutagenesis of a protein kinase identifies functional regions involved in catalysis and substrate interactions. J. Biol. Chem. **266**, 8923–8931 PubMed

60 Bailey, F.P., Byrne, D.P., McSkimming, D., Kannan, N. and Eyers, P.A. (2015) Going for broke: targeting the human cancer pseudokinome1. Biochem. J. **465**, 195–211 CrossRef PubMed

61 Fedorov, O., Muller, S. and Knapp, S. (2010) The (un)targeted cancer kinome. Nat. Chem. Biol. **6**, 166–169 CrossRef PubMed

62 Knapp, S., Arruda, P., Blagg, J., Burley, S., Drewry, D.H., Edwards, A., Fabbro, D., Gillespie, P., Gray, N.S., Kuster, B. et al. (2013) A public-private partnership to unlock the untargeted kinome. Nat. Chem. Biol. **9**, 3–6 CrossRef PubMed

63 Cohen, P. and Alessi, D.R. (2013) Kinase drug discovery–what's next in the field? ACS Chem. Biol. **8**, 96–104 CrossRef PubMed

64 Bishop, A.C., Ubersax, J.A., Petsch, D.T., Matheos, D.P., Gray, N.S., Blethrow, J., Shimizu, E., Tsien, J.Z., Schultz, P.G., Rose, M.D. et al. (2000) A chemical switch for inhibitor-sensitive alleles of any protein kinase. Nature **407**, 395–401 CrossRef PubMed

65 Good, N.E., Winget, G.D., Winter, W., Connolly, T.N., Izawa, S. and Singh, R.M. (1966) Hydrogen ion buffers for biological research. Biochemistry **5**, 467–477 CrossRef PubMed

66 Williams, T.I., Combs, J.C., Thakur, A.P., Strobel, H.J. and Lynn, B.C. (2006) A novel bicine running buffer system for doubled sodium dodecyl sulfate - polyacrylamide gel electrophoresis of membrane proteins. Electrophoresis **27**, 2984–2995 CrossRef PubMed

67 Yang, J., Wu, J., Steichen, J.M., Kornev, A.P., Deal, M.S., Li, S., Sankaran, B., Woods, Jr, V.L. and Taylor, S.S. (2012) A conserved Glu-Arg salt bridge connects coevolved motifs that define the eukaryotic protein kinase fold. J. Mol. Biol. **415**, 666–679 CrossRef PubMed

68 Kato, H., Gotoh, H., Kajikawa, M. and Suto, K. (1998) Depolarization triggers intracellular magnesium surge in cultured dorsal root ganglion neurons. Brain Res. **779**, 329–333 CrossRef PubMed

69 Bozym, R.A., Thompson, R.B., Stoddard, A.K. and Fierke, C.A. (2006) Measuring picomolar intracellular exchangeable zinc in PC-12 cells using a ratiometric fluorescence biosensor. ACS Chem. Biol. **1**, 103–111 CrossRef PubMed

70 Hartwig, A. (2001) Role of magnesium in genomic stability. Mutat. Res. **475**, 113–121 CrossRef PubMed

71 Qin, Y., Miranda, J.G., Stoddard, C.I., Dean, K.M., Galati, D.F. and Palmer, A.E. (2013) Direct comparison of a genetically encoded sensor and small molecule indicator: implications for quantification of cytosolic Zn(2 +). ACS Chem. Biol. **8**, 2366–2371 CrossRef PubMed

72 Eyers, P.A., Liu, J., Hayashi, N.R., Lewellyn, A.L., Gautier, J. and Maller, J.L. (2005) Regulation of the G(2)/M transition in *Xenopus* oocytes by the cAMP-dependent protein kinase. J. Biol. Chem. **280**, 24339–24346 CrossRef PubMed

73 Cameron, A.J., Escribano, C., Saurin, A.T., Kostelecky, B. and Parker, P.J. (2009) PKC maturation is promoted by nucleotide pocket occupation independently of intrinsic kinase activity. Nat. Struct. Mol. Biol. **16**, 624–630 CrossRef PubMed

74 Zeqiraj, E., Filippi, B.M., Deak, M., Alessi, D.R. and van Aalten, D.M.F. (2009) Structure of the LKB1-STRAD-MO25 complex reveals an allosteric mechanism of kinase activation. Science **326**, 1707–1711 CrossRef PubMed

75 Hildebrand, J.M., Tanzer, M.C., Lucet, I.S., Young, S.N., Spall, S.K., Sharma, P., Pierotti, C., Garnier, J.M., Dobson, R.C., Webb, A.I. et al. (2014) Activation of the pseudokinase MLKL unleashes the four-helix bundle domain to induce membrane localization and necroptotic cell death. Proc. Natl. Acad. Sci. U.S.A. **111**, 15072–15077 CrossRef PubMed

76 Murphy, J.M., Czabotar, P.E., Hildebrand, J.M., Lucet, I.S., Zhang, J.G., Alvarez-Diaz, S., Lewis, R., Lalaoui, N., Metcalf, D., Webb, A.I. et al. (2013) The pseudokinase MLKL mediates necroptosis via a molecular switch mechanism. Immunity **39**, 443–453 CrossRef PubMed

77 Jung, C.H., Ro, S.H., Cao, J., Otto, N.M. and Kim, D.H. (2010) mTOR regulation of autophagy. FEBS Lett. **584**, 1287–1295 CrossRef PubMed

78 Liang, C. and Jung, J.U. (2010) Autophagy genes as tumor suppressors. Curr. Opin. Cell Biol. **22**, 226–233 CrossRef PubMed

79 Min, X., Lee, B.H., Cobb, M.H. and Goldsmith, E.J. (2004) Crystal structure of the kinase domain of WNK1, a kinase that causes a hereditary form of hypertension. Structure **12**, 1303–1311 CrossRef PubMed

80 Piala, A.T., Moon, T.M., Akella, R., He, H., Cobb, M.H. and Goldsmith, E.J. (2014) Chloride sensing by WNK1 involves inhibition of autophosphorylation. Sci. Signal. **7**, ra41 PubMed

81 Lang, B., Pu, J., Hunter, I., Liu, M., Martin-Granados, C., Reilly, T.J., Gao, G.D., Guan, Z.L., Li, W.D., Shi, Y.Y. et al. (2014) Recurrent deletions of ULK4 in schizophrenia: a gene crucial for neuritogenesis and neuronal motility. J. Cell Sci. **127**, 630–640 CrossRef PubMed

82 Broderick, P., Chubb, D., Johnson, D.C., Weinhold, N., Forsti, A., Lloyd, A., Olver, B., Ma, Y.P., Dobbins, S.E., Walker, B.A. et al. (2012) Common variation at 3p22.1 and 7p15.3 influences multiple myeloma risk. Nat. Genet. **44**, 58–61 CrossRef

83 Vogel, P., Read, R.W., Hansen, G.M., Payne, B.J., Small, D., Sands, A.T. and Zambrowicz, B.P. (2012) Congenital hydrocephalus in genetically engineered mice. Vet. Pathol. **49**, 166–181 CrossRef PubMed

84 Hari, S.B., Merritt, E.A. and Maly, D.J. (2014) Conformation-selective ATP-competitive inhibitors control regulatory interactions and noncatalytic functions of mitogen-activated protein kinases. Chem. Biol. **21**, 628–635 CrossRef PubMed

85 Chen, C., Ha, B.H., Thevenin, A.F., Lou, H.J., Zhang, R., Yip, K.Y., Peterson, J.R., Gerstein, M., Kim, P.M., Filippakopoulos, P. et al. (2014) Identification of a major determinant for serine-threonine kinase phosphoacceptor specificity. Mol. Cell **53**, 140–147 CrossRef PubMed

86 Pao, W., Miller, V., Zakowski, M., Doherty, J., Politi, K., Sarkaria, I., Singh, B., Heelan, R., Rusch, V., Fulton, L. et al. (2004) EGF receptor gene mutations are common in lung cancers from "never smokers" and are associated with sensitivity of tumors to gefitinib and erlotinib. Pro. Natl. Acad. Sci. U.S.A. **101**, 13306–13311 CrossRef

87 Girdler, F., Gascoigne, K.E., Eyers, P.A., Hartmuth, S., Crafter, C., Foote, K.M., Keen, N.J. and Taylor, S.S. (2006) Validating Aurora B as an anti-cancer drug target. J. Cell Sci. **119**, 3664–3675 CrossRef PubMed

88 Elphick, L.M., Lee, S.E., Child, E.S., Prasad, A., Pignocchi, C., Thibaudeau, S., Anderson, A.A., Bonnac, L., Gouverneur, V. and Mann, D.J. (2009) A quantitative comparison of wild-type and gatekeeper mutant cdk2 for chemical genetic studies with ATP analogues. Chembiochem **10**, 1519–1526 CrossRef PubMed

89 Huang, D., Zhang, Y. and Chen, X. (2003) Analysis of intracellular nucleoside triphosphate levels in normal and tumor cell lines by high-performance liquid chromatography. J. Chromatogr. B Analyt. Technol. Biomed. Life Sci. **784**, 101–109 CrossRef PubMed

90 Garske, A.L., Peters, U., Cortesi, A.T., Perez, J.L. and Shokat, K.M. (2011) Chemical genetic strategy for targeting protein kinases based on covalent complementarity. Proc. Natl. Acad. Sci. U.S.A. **108**, 15046–15052 CrossRef PubMed

91 Davis, M.I., Hunt, J.P., Herrgard, S., Ciceri, P., Wodicka, L.M., Pallares, G., Hocker, M., Treiber, D.K. and Zarrinkar, P.P. (2011) Comprehensive analysis of kinase inhibitor selectivity. Nat. Biotechnol. **29**, 1046–1051 CrossRef PubMed

92 Bantscheff, M., Eberhard, D., Abraham, Y., Bastuck, S., Boesche, M., Hobson, S., Mathieson, T., Perrin, J., Raida, M., Rau, C. et al. (2007) Quantitative chemical proteomics reveals mechanisms of action of clinical ABL kinase inhibitors. Nat. Biotechnol. **25**, 1035–1044 CrossRef PubMed

93 Bailey, F.P., Andreev, V.I. and Eyers, P.A. (2014) The resistance tetrad: amino acid hotspots for kinome-wide exploitation of drug-resistant protein kinase alleles. Methods Enzymol. **548**, 117–146 CrossRef PubMed

94 Bishop, A.C., Shah, K., Liu, Y., Witucki, L., Kung, C. and Shokat, K.M. (1998) Design of allele-specific inhibitors to probe protein kinase signaling. Curr. Biol. **8**, 257–266 CrossRef PubMed

95 Liu, Q., Sabnis, Y., Zhao, Z., Zhang, T., Buhrlage, S.J., Jones, L.H. and Gray, N.S. (2013) Developing irreversible inhibitors of the protein kinase cysteinome. Chem. Biol. **20**, 146–159 CrossRef PubMed

96 Cohen, M.S., Zhang, C., Shokat, K.M. and Taunton, J. (2005) Structural bioinformatics-based design of selective, irreversible kinase inhibitors. Science **308**, 1318–1321 CrossRef PubMed

97   Xie, T., Lim, S.M., Westover, K.D., Dodge, M.E., Ercan, D., Ficarro, S.B., Udayakumar, D., Gurbani, D., Tae, H.S., Riddle, S.M. et al. (2014) Pharmacological targeting of the pseudokinase Her3. Nat. Chem. Biol. **10**, 1006–1012 CrossRef PubMed

98   Salazar, M., Lorente, M., Garcia-Taboada, E., Perez Gomez, E., Davila, D., Zuniga-Garcia, P., Maria Flores, J., Rodriguez, A., Hegedus, Z., Mosen-Ansorena, D. et al. (2014) Loss of tribbles pseudokinase-3 promotes Akt-driven tumorigenesis via FOXO inactivation. Cell. Death Differ. **22**, 131–144 CrossRef PubMed

99   Yokoyama, T., Kanno, Y., Yamazaki, Y., Takahara, T., Miyata, S. and Nakamura, T. (2010) Trib1 links the MEK1/ERK pathway in myeloid leukemogenesis. Blood **116**, 2768–2775 CrossRef PubMed

100 Du, K., Herzig, S., Kulkarni, R.N. and Montminy, M. (2003) TRB3: a tribbles homolog that inhibits Akt/PKB activation by insulin in liver. Science **300**, 1574–1577 CrossRef PubMed

101 Grandinetti, K.B., Stevens, T.A., Ha, S., Salamone, R.J., Walker, J.R., Zhang, J., Agarwalla, S., Tenen, D.G., Peters, E.C. and Reddy, V.A. (2011) Overexpression of TRIB2 in human lung cancers contributes to tumorigenesis through downregulation of C/EBPα. Oncogene **30**, 3328–3335 CrossRef PubMed

102 Hsu, P.D., Lander, E.S. and Zhang, F. (2014) Development and applications of CRISPR-Cas9 for genome engineering. Cell **157**, 1262–1278 CrossRef PubMed

103 Claus, J., Cameron, A.J. and Parker, P.J. (2013) Pseudokinase drug intervention: a potentially poisoned chalice. Biochem. Soc. Trans. **41**, 1083–1088 CrossRef PubMed

104 Amin, D.N., Sergina, N., Ahuja, D., McMahon, M., Blair, J.A., Wang, D., Hann, B., Koch, K.M., Shokat, K.M. and Moasser, M.M. (2010) Resiliency and vulnerability in the HER2-HER3 tumorigenic driver. Sci. Transl. Med. **2**, 16ra17 PubMed

105 Littlefield, P., Moasser, M.M. and Jura, N. (2014) An ATP-competitive inhibitor modulates the allosteric function of the HER3 pseudokinase. Chem. Biol. **21**, 453–458 CrossRef PubMed

106 Zanella, F., Renner, O., Garcia, B., Callejas, S., Dopazo, A., Peregrina, S., Carnero, A. and Link, W. (2010) Human TRIB2 is a repressor of FOXO that contributes to the malignant phenotype of melanoma cells. Oncogene **29**, 2973–2982 CrossRef PubMed

107 Wang, J., Park, J.-S., Wei, Y., Rajurkar, M., Cotton, J.L., Fan, Q., Lewis, B.C., Ji, H. and Mao, J. (2013) TRIB2 acts downstream of Wnt/TCF in liver cancer cells to regulate YAP and C/EBPα function. Mol. Cell **51**, 211–225 CrossRef PubMed